Science of the Total Environment 897 (2023) 165144

Contents lists available at ScienceDirect

Science of the Total Environment

journal homepage: www.elsevier.com/locate/scitotenv

Intimately tracking NO_2 pollution over the New York City - Long Island Sound land-water continuum: An integration of shipboard, airborne, satellite observations, and models

Maria Tzortziou [a,b,*], Christopher P. Loughner [c], Daniel L. Goldberg [d], Laura Judd [e], Dilchand Nauth [a], Charlotte F. Kwong [a], Tong Lin [a], Alexander Cede [b,f,g], Nader Abuhassan [b,g,h]

[a] Earth & Atmospheric Sciences, City College of New York, New York, NY 10031, USA
[b] NASA Goddard Space Flight Center, Greenbelt, MD 20771, USA
[c] NOAA Air Resources Laboratory, College Park, MD 20740, USA
[d] Department of Environmental and Occupational Health, George Washington University, Washington, DC 20052, USA
[e] NASA Langley Research Center, Hampton, VA 23681, USA
[f] LuftBlick, Kreith, Austria
[g] SciGlob Instruments and Services LLC, Columbia, MD 21046, USA
[h] Joint Center for Earth Systems Technology, University of Maryland, Baltimore, MD 21201, USA

HIGHLIGHTS

- Multiplatform observations uniquely track NO_2 dynamics across land-water continuum.
- Aircraft $TCNO_2$ retrievals were in excellent agreement with Pandora measurements.
- TROPOMI underestimated $TCNO_2$ particularly over the highly dynamic NY coastal waters.
- Changes in $TCNO_2$ by more than a factor of three during sea breeze events
- Urban NO_2 pollution plumes extended >30 km over LIS under low speed westerly winds.

GRAPHICAL ABSTRACT

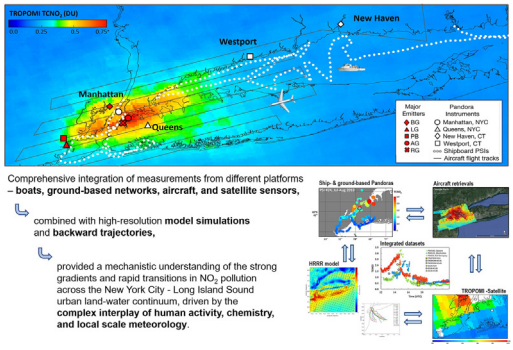

ARTICLE INFO

Editor: Anastasia Paschalidou

Keywords:
Remote sensing
Shipborne measurements
NO_2
Urban air-quality
Sea breezes
Land-water continuum
Satellite retrievals
Aircraft retrievals
Model simulations

ABSTRACT

Nitrogen dioxide (NO_2) pollution remains a serious global problem, particularly near highly populated urbanized coasts that face increasing challenges with climate change. Yet, the combined impact of urban emissions, pollution transport, and complex meteorology on the spatiotemporal dynamics of NO_2 along heterogeneous urban coastlines remains poorly characterized. Here, we integrated measurements from different platforms – boats, ground-based networks, aircraft, and satellites – to characterize total column NO_2 ($TCNO_2$) dynamics across the land-water continuum in the New York metropolitan area, the most populous area in the United States that often experiences the highest national NO_2 levels. Measurements were conducted during the 2018 Long Island Sound Tropospheric Ozone Study (LISTOS), with a main goal to extend surface measurements beyond the coastline – where ground-based air-quality monitoring networks abruptly stop – and over the aquatic environment where peaks in air pollution often occur. Satellite $TCNO_2$ from TROPOMI correlated strongly with Pandora surface measurements (r = 0.87, N = 100) both over land and water. Yet, TROPOMI overall underestimated $TCNO_2$ (MPD = -12%) and missed peaks in NO_2 pollution caused by rush hour emissions or pollution accumulation during sea breezes. Aircraft retrievals were in excellent agreement with Pandora (r = 0.95, MPD = -0.3%, N = 108). Stronger agreement was found between

* Corresponding author at: Earth & Atmospheric Sciences, City College of New York, New York, NY 10031, USA.
E-mail address: mtzortziou@ccny.cuny.edu (M. Tzortziou).

http://dx.doi.org/10.1016/j.scitotenv.2023.165144
Received 28 March 2023; Received in revised form 23 June 2023; Accepted 24 June 2023
Available online 29 June 2023

TROPOMI, aircraft, and Pandora over land, while over water satellite, and to a lesser extent aircraft, retrievals underestimated $TCNO_2$ particularly in the highly dynamic New York Harbor environment. Combined with model simulations, our shipborne measurements uniquely captured rapid transitions and fine-scale features in NO_2 behavior across the New York City - Long Island Sound land-water continuum, driven by the complex interplay of human activity, chemistry, and local scale meteorology. These novel datasets provide critical information for improving satellite retrievals, enhancing air quality models, and informing management decisions, with important implications for the health of diverse communities and vulnerable ecosystems along this complex urban coastline.

1. Introduction

A human fingerprint on global air quality, nitrogen dioxide (NO_2) pollution remains a serious problem in many major cities worldwide (e.g., Rojas and Venegas, 2009; Gu et al., 2011; Chi et al., 2021;; Tzortziou et al., 2022). Emitted to the atmosphere primarily during fossil fuel combustion, NO_2 is a criteria air pollutant that is regulated and monitored by the Clean Air Act because of its direct effects on human and environmental health and its major role as a precursor of ozone and secondary inorganic aerosols (Crutzen, 1979; Burnett et al., 2004; Duan et al., 2019). High NO_2 levels have been associated with lung irritation and reduced lung function, increased asthma attacks, cardiovascular disorders, as well as lower birth weight in newborns and increased risk of premature death (U.S. EPA, 2016). Through wet and dry deposition, the atmosphere is a major source of excess nitrogen to many terrestrial and aquatic ecosystems worldwide (Paerl et al., 2002; Pardo et al., 2011). Prior studies have indicated atmospheric deposition accounts for 25% or more of the annual nitrogen load to systems such as the Chesapeake Bay and Long Island Sound, with important implications for soil biogeochemistry, aquatic biology, development of coastal eutrophication, harmful algal blooms, and hypoxia (e.g., Stacey et al., 2001; Decina et al., 2017; Decina et al., 2020; Burns et al., 2021).

Strict air quality regulation policies (e.g., Clean Air Interstate Rule, CAIR, 2009) over the past two decades, addressing regional interstate transport of fine particulate matter and ozone, have resulted in consistent and significant declines in nitrogen oxide ($NOx = NO + NO_2$) emissions across the United States (Van Der A et al., 2008; Duncan et al., 2016; Krotkov et al., 2016). Satellite observations from the Ozone Monitoring Instrument (OMI) captured an approximately 4% yr^{-1} decrease in column NO_2 levels between 2005 and 2019 over the eastern US (Krotkov et al., 2016; Goldberg et al., 2021). Yet, many US cities remain hot spots of NO_2 pollution (Goldberg et al., 2021), depicting clear NO_2 weekly cycles and interannual variability strongly linked to human behavior (Beirle et al., 2003; Kaynak et al., 2009; Tzortziou et al., 2022).

Home to approximately 6% of the United States' population (U.S. Census Bureau, 2021) the New York City metropolitan area is the most populous urban center in the United States. Despite satellite Aura/OMI observations showing a ~ 3.8% yr^{-1} drop in total column NO_2 over New York City (NYC) between 2005 and 2019 (Tzortziou et al., 2022) and a 46% decline in top-down NO_X emissions from 2006 to 2017 (Goldberg et al., 2019a), this coastal metropolis continues to experience among the highest national NO_2 levels (Herman et al., 2018). As a result, this area has the worst nonattainment records of ozone in eastern North America (Karambelas, 2020). These high levels of pollution impact the well-being of over 20 million people living in the New York metropolitan region, affecting the health of diverse, including many low-income disadvantaged, communities and already vulnerable ecosystems in downwind areas (Clark et al., 2014).

Air quality exceedances in New York are the result of local and regional anthropogenic pollutant emissions from various sectors (e.g., transportation, energy, industrial) as well as meteorological conditions influenced by a complex land-water interface and heterogeneous terrain (Couillard et al., 2021; Tzortziou et al., 2022). In this and other coastal urban areas, air pollution from urban cores often accumulates over adjacent coastal waters due to low atmospheric deposition rates over water and a shallow marine boundary layer that traps urban and marine emissions (Goldberg et al., 2014; Loughner et al., 2016). Sea-breeze circulations that often develop across large bodies of water, such as the Mid-Atlantic Bight and Long Island Sound, further affect advection, recirculation, and accumulation of atmospheric pollutants. Such sea-breeze flows can lead to build up of emissions and aggravation of air pollution along the shoreline caused by stagnation that develops as winds change direction (Gaza, 1998; Kanakidou et al., 2011; Stauffer et al., 2014; Loughner et al., 2016). Although sea breeze events do not occur every day, their frequency, duration, and severity are expected to increase with coastal urbanization and climate change (Leung and Gustafson, 2005; Zhang et al., 2009; Horton et al., 2012). Previous studies have examined the development of sea and shore breeze circulations along the coasts of Long Island Sound (LIS) and NY Harbor (Colle and Novak, 2010; Meir et al., 2013; Thompson et al., 2007). Yet, the combined impact of such meteorological processes and different NOx emission sectors on the spatiotemporal dynamics of NO_2 along this complex urban coastline remains poorly characterized –particularly across the *continuum of terrestrial and aquatic landscapes* already stressed by pollution, eutrophication, and rising temperatures.

The 2018 Long Island Sound Tropospheric Ozone Study (LISTOS) was a large multi-agency collaborative effort led by the Northeast States for Coordinated Air Use Management (NESCAUM) to better understand the complex chemistry and pollution transport in this region (Karambelas, 2020). A main goal of LISTOS was to characterize the sources and dynamics of the ozone precursors nitrogen oxides (NOx) and volatile organic compounds (VOCs) and improve understanding of pollution transport from NYC and upwind regions to downwind areas and over Long Island Sound (http://www.nescaum.org/documents/listos). Several academic and research institutions, local state agencies, and federal agencies participated, contributing measurements from surface networks, mobile laboratories, research aircraft, and satellite sensors in summer 2018 (e.g., Judd et al., 2020; Zhang et al., 2021; Rogers et al., 2020; Wu et al., 2021; Couillard et al., 2021).

The overarching objective of our study was to extend the LISTOS surface measurements of NO_2 beyond the coastline – where ground-based air-quality monitoring networks abruptly stop – and over the aquatic environment where peaks in air pollution often occur. Shipboard Pandora spectrometer instruments, specifically designed for accurate and high-frequency retrievals of atmospheric trace gas column amounts from a moving platform, were, thus, deployed on two research vessels conducting regular year-round water-quality monitoring surveys in New York Harbor and across Long Island Sound. These novel datasets provide unique information for validating satellite and aircraft column NO_2 retrievals over highly heterogeneous coastal waters. They are also critical for evaluating atmospheric correction approaches for satellite ocean color observations (Tzortziou et al., 2018; Turner et al., 2022). Combined with model simulations and measurements from airborne, satellite, and land-based instruments, the shipboard Pandora retrievals allowed to characterize rapid transitions and fine-scale features in NO_2 behavior across the NYC-LIS urban land-water continuum, driven by the complex interplay of human activity, chemistry, and local scale meteorology.

2. Data and methods

2.1. Ground-based and shipboard Pandora measurements

To characterize the spatiotemporal dynamics in total column NO_2 ($TCNO_2$) across the NYC-LIS urban-land-water continuum we used high-

frequency measurements from both shipboard and ground-based Pandora spectrometer instruments (PSIs) deployed on mobile research vessels and at fixed coastal land sites (Fig. 1; Table 1). In this study, we discuss measurements collected in July through September 2018, which was during the peak activity of the LISTOS field campaign. The Pandora sensors are part of the Pandonia Global Network (PGN, https://www.pandonia-global-network.org/), jointly sponsored by the National Aeronautics and Space Administration (NASA) and the European Space Agency (ESA). The PGN provides real-time, standardized, calibrated, and verified air quality data from a network of passive remote sensing instruments capable of performing sun, moon, and sky observations. PGN measurements have been used extensively in support of air quality monitoring and satellite validation (e.g., Celarier et al., 2008; Reed et al., 2015; Tzortziou et al., 2018; Spinei et al., 2018; Herman et al., 2019; Di Bernardino et al., 2021; Verhoelst et al., 2021). Recent studies have combined model simulations with long-term data records from ground-based Pandora instruments to assess impacts of the COVID-19 pandemic on air quality in the New York metropolitan area (Tzortziou et al., 2022), as well as to validate NASA airborne measurements and TROPOMI NO_2 retrievals over land during LISTOS (Judd et al., 2020) and other major field campaigns (Choi et al., 2020).

Pandora is a sun/sky/lunar passive UV/Visible spectrometer system, driven by a highly accurate sun tracker that points an optical head at the sun and transmits the received light to an Avantes low stray light CCD spectrometer (spectral range: 280–525 nm; spectral resolution: 0.6 nm with 5 times oversampling) through a fiber optic cable (Herman et al., 2019; Tzortziou et al., 2014). The spectrometer is temperature stabilized at 20 °C inside a weather resistant container. Trace gas abundances along the light path are determined using differential optical absorption spectroscopy (DOAS). The system can operate in both direct-sun and sky-scan mode for retrievals of O_3, NO_2, SO_2 and CH_2O total columns, tropospheric columns, and information on vertical profiles (Tzortziou et al., 2018; Herman et al., 2018; Spinei et al., 2018), and is an enhanced monitoring instrument for characterizing upper air pollutants under the U.S. EPA PAMS program (Szykman et al., 2019). For the shipboard instruments, the Blick Software suite operating the PSI uses feedback from an internal digital camera to a sun-tracker to adjust the motors and maintain a centered direct-sun view (Tzortziou et al., 2018). The estimated $TCNO_2$ error in Pandora retrievals is <0.05 DU (1 DU = 2.69×10^{16} molecules cm^{-2}) (Herman et al., 2019). Pandora data were filtered here for solar zenith angle (SZA) less than 70°, normalized root-mean square (nRMS) of weighted spectral fitting residuals <0.05, and uncertainty in NO_2 retrievals <0.1 DU.

PGN sites in the New York City and Long Island Sound region during LISTOS included Manhattan, NY (PSI#135), Queens, NY (PSI#140), Westport, CT (PSI#53), and New Haven, CT (PSI#20) (Table 1, Fig. 1). PSI#135 is located in Upper West Manhattan, NY, on the Advanced Science Research Center (ASRC) Rooftop Observatory at the City College of New York campus, an intensive urban air-quality monitoring site. The Pandora sensor in Queens, NY, is located at the CUNY Queens College, a New York Department of Environmental Conservation (NYDEC) Air Toxics and NCore monitoring site within a dense residential neighborhood and near several major roadways. The Pandora in New Haven, CT, is located at the Connecticut Department of Energy and Environmental Protection (CT-DEEP) Photochemical Assessment Monitoring Station (PAMS) in Criscuolo Park, at the confluence of the Mill and Quinnipiac Rivers surrounded by a residential neighborhood near the elevated intersection of three major highways and industrial activities across the rivers. The Pandora in Westport, CT, is located at the Westport Sherwood Island State Park site in southwestern Connecticut. This is a rural coastal site that is approximately 0.5 km to the south of I-95 on the Long Island Sound shoreline.

During LISTOS 2018, two shipboard Pandora sensors collected measurements of atmospheric trace gases in NY Harbor and across Long Island Sound (Fig. 1). PSI#24, was deployed on the 55-ft *HSV Osprey*, operated by the NYC Department of Environmental Protection (DEP) as part of their New York Harbor Survey Program (18 July-15 August 2018). NYC DEP has been conducting long-term (1909-now) water quality measurements in the Hudson River, East River, Inner Harbor, Lower NY Bay, Jamaica Bay, and Western LIS weekly from June to September and once a month during the rest of the year. Shipboard PSI#100, was deployed on the 50-ft *R/V John Dempsey*, operated by the CT Department of Energy and Environmental Protection (DEEP) (23 August-5 September 2018). Since 1991, CT-DEEP has conducted an intensive year-round water quality monitoring program across the Eastern to Western Long Island Sound, funded by the US EPA Long Island Sound Study, with bi-weekly surveys during summer months. Both shipboard Pandora instruments were mounted on the bow/forecastle deck of the research vessels, away from the engine's exhaust, to avoid any obstructions and contamination.

2.2. TROPOMI satellite retrievals

Jointly developed by the Netherlands and ESA, TROPOMI is an air quality monitoring sensor onboard the sun-synchronous Copernicus Sentinel-5 Precursor satellite, launched on 13 October 2017 (Veefkind et al., 2012). On a low-earth (825 km) orbit, Sentinel-5P has a daily equator overpass time of approximately 13:30 local time and global daily coverage. TROPOMI has a spatial resolution of 7.2 km (5.6 km as of 6 August 2019) along-track by 3.6 km across-track at nadir, a significant improvement compared to its predecessors OMI (Ozone Monitoring Instrument) and SCIAMACHY (SCanning Imaging Absorption spectroMeter for Atmospheric

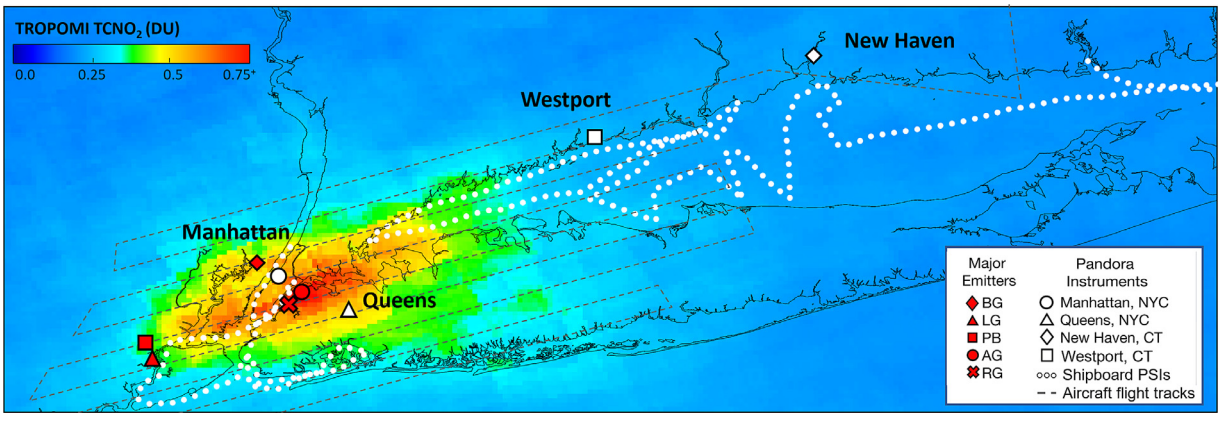

Fig. 1. Map of study area, indicating location of ground-based and shipborne Pandora sensors (white symbols) in New York City, NY Harbor, Connecticut, and Long Island Sound, as well as aircraft flight tracks (grey dash line), overlaid with mean August 2018 total column NO_2 from TROPOMI (in DU). Major pollutant emitters in the area are included (red symbols), specifically the PSEG Bergen Generating Station in Ridgefield (BG), the Linden Generating Station (LG) and the Phillips 66 Bayway (PB) Refinery in Linden (major emission sources in NJ), and the Astoria (AG) and Ravenswood Generating (RG) Stations in Queens, NY (among the largest greenhouse gas polluters in the state of NY in 2018 and 2019; Tzortziou et al., 2022).

Table 1
Pandora sites and instruments used in this study. The mean (and standard deviation, stdev) $TCNO_2$ amount (based on half-hour averages, July–September 2018) at each site during LISTOS is also shown.

Pandora sites (Principal Investigator)	PSI #	Latitude	Longitude	$TCNO_2$ during LISTOS (DU, mean, ± stdev)
Manhattan, NY (M. Tzortziou)	#135	40.8153°	−73.9505°	0.59 (± 0.32)
Queens, NY (L. Valin)	#140	40.7361°	−73.8215°	0.54 (± 0.30)
Westport, CT (L. Valin)	#53	41.1183°	−73.3367°	0.27 (± 0.08)
New Haven, CT (L. Valin)	#20	41.3014°	−72.9029°	0.33 (± 0.09)
Shipboard NYC-DEP (M. Tzortziou)	#24	40.4842° to 40.9145°	−74.2592° to −73.7469°	0.91 (± 0.45)
Shipboard CT-DEEP (M. Tzortziou)	#100	40.8718° to 41.3126°	−73.7363° to −72.0494°	0.28 (± 0.05)

CartograpHY). Several spectral bands in the ultraviolet to shortwave-infrared (270–2385 nm) and a spectral resolution between 0.25 and 1 nm, allow observations of cloud, aerosol properties, and key atmospheric trace gases including O_3, NO_2, CO, SO_2, CH_4 and CH_2O (Veefkind et al., 2012). NO_2 retrievals from TROPOMI are based on measurements in the 405–465 nm spectral window. Using a DOAS technique, similar to the Pandora instrument, the top-of-atmosphere spectral radiances are converted into slant column amounts of NO_2 between the sensor and the Earth's surface (Boersma et al., 2018). In two additional steps, subtraction of the stratospheric component and incorporation of an air mass factor, the slant column quantity is converted into a tropospheric vertical column content (Beirle et al., 2019; Dix et al., 2020; Goldberg et al., 2019b; Griffin et al., 2019; Ialongo et al., 2020; Reuter et al., 2019; Zhao et al., 2020; van Geffen et al., 2022). For this analysis, we used the TROPOMI total vertical columns (tropospheric and stratospheric column amount, in Dobson units) using TROPOMI NO_2 version 2.3.1 (https://data-portal.s5p-pal.com/). TROPOMI data were filtered using a quality assurance flag (QA), in which pixels with QA values >0.75 are utilized; no other filter was applied.

2.3. Aircraft NO_2 retrievals

Over the course of the LISTOS study, NASA flew two ultraviolet-visible (UV-VIS) airborne spectrometers: the Geostationary Coastal and Air Pollution Events Airborne Simulator (GCAS) from July–September 2018 and Geostationary Trace gas and Aerosol Sensor Optimization (GeoTASO) in June 2018 (Kowalewski and Janz, 2014; Leitch et al., 2014). The data from these spectrometers were used to retrieve high resolution maps of NO_2 and formaldehyde, the former used in the following analysis with a spatial resolution of approximately 250 m × 250 m on 13 flight days. Brief details about the flight strategy, retrieval, and validation are summarized below with more detailed descriptions in Judd et al. (2020) and references therein. NO_2 is retrieved via DOAS in the 425–460 nm window. Air mass factors (AMFs) for slant to vertical column conversion rely on a priori input based on surface reflectivity from MODIS BRDF kernels (MCD41A1: Lucht et al., 2000; Schaaf and Wang, 2015) over land with assumed Lambertian reflectance of at least 3% (or larger if the MODIS retrieval indicated otherwise) plus a Cox-Munk kernel for sun glint approximation over water, a priori profiles from a 12 km NAM-CMAQ modeling analysis for the troposphere (Stajner et al., 2011) plus the PRATMO stratospheric climatology (Prather, 1992; McLinden et al., 2000) bias corrected daily with TROPOMI 1.3 stratospheric vertical columns. Both airborne instruments have a field of view nadir of the aircraft of 45°, resulting in an approximate 7 km swath width at a flight altitude of 8.5 km. Maps of NO_2 are composed by executing flight lines in a lawnmower pattern across the region of interest between 2 and 4 times per flight day over the region over a time period of approximately 1.5–3 h. Previous work and data shown herein demonstrate that this airborne dataset compares well with Pandora spectrometers to within ± 25%, which exceeds most independent estimates of uncertainty in relation to AMF applications for slant to vertical column conversion (Lorente et al., 2017). Data in this work are filtered to only include cloud-free scenes.

2.4. HYSPLIT model simulations

The NOAA Air Resources Laboratory (ARL) HYbrid Single-Particle Lagrangian Integrated Trajectory (HYSPLIT) modeling system was used to compute air parcel trajectories and determine the origin of air masses sampled by the shipboard Pandoras during LISTOS. HYSPLIT is a complete system capable of computing air parcel trajectories, atmospheric dispersion, emissions, chemical transformation, and deposition within Earth's atmosphere (Stein et al., 2015). It has been used extensively in the literature in a wide range of applications to simulate and forecast the atmospheric transport, dispersion, and deposition of pollutants emitted from stationary and mobile sources, hazardous materials, wildfire smoke, and volcanic ash (e.g., Stein et al., 2015; Rolph et al., 2017; Nauth et al., 2023). HYSPLIT was previously used successfully to compute the transport and origin of air masses sampled by a shipboard Pandora (PSI#24) onboard *R/V Onnuri* during the Korea-United States Ocean Color (KORUS-OC) expedition in South Korean coastal waters (Tzortziou et al., 2018). For this study, HYSPLIT backward trajectories were initialized at 18:00 UTC for each day between 1 July to 31 August 2018 and driven by the HRRR meteorological model. The trajectories were initialized at 500 m AGL (above ground level) and run 12 h backward in time with a model top of 10,000 m AGL. HYSPLIT default options were used for the remaining options, which include using the vertical velocity from the meteorological inputs, in this case HRRR calculated vertical velocity, and outputting the location of the trajectories on an hourly basis. Results were analyzed in combination with HRRR model simulations of wind conditions to assess source contributions to atmospheric pollution over these coastal waters and impacts of sea breeze circulations during the LISTOS field campaign.

2.5. HRRR model simulations

The High-Resolution Rapid Refresh (HRRR) atmospheric model, developed by the NOAA Earth System Research Laboratory (ESRL), was used in this study to drive the HYSPLIT model simulations. The HRRR model is a real-time 3-km resolution, hourly updated, cloud-resolving, convection-allowing atmospheric model, initialized by 3 km grids with 3 km radar assimilation and 50 vertical levels (Alexander, 2021). Radar data is assimilated in the HRRR every 15 min over a 1-h period adding further detail to that provided by the hourly data assimilation from the 13 km radar-enhanced Rapid Refresh. Previous research has shown that meteorological models with a horizontal resolution coarser than about 4.5 km may not be capable of capturing sea breeze circulations (Loughner et al., 2011). The HRRR model has a high enough (i.e., 3 km) spatial resolution to capture these localized circulation patterns. With the influence of onshore and offshore surface winds over the NYC metropolitan area, HRRR

provides detailed products allowing for the further analysis of wind patterns that affect the movement of polluted air parcels over the area (Nauth et al., 2023). The HRRR model 10 m wind velocities were used to identify sea breeze convergence zones. Strong sea breezes, when the sea breeze penetrated far inland, as well as weak sea breezes, when the convergence zone was identified along the coastline but did not penetrate far inland, were counted as sea breeze days (Nauth et al., 2023).

2.6. $TCNO_2$ statistical comparison methods

Linear regression statistics (including the correlation coefficient *r*) were used to examine the correlation between coincident satellite, aircraft, and Pandora retrievals. Mean percent differences (MPD) in total column NO_2 amounts were calculated with Pandora retrievals as the reference, using Eq. (1).

$$Mean\ PD\ (MPD) = \left\{ \sum_{i=1}^{N} \left(\frac{\left[X_i^{Satellite\ or\ Aircraft} - X_i^{PSI} \right]}{X_i^{PSI}} \right) \right\} \times 100/N \quad (1)$$

where $X_i^{Satellite}$ $X_i^{Aircraft}$ and X_i^{PSI} are the satellite, aircraft, and Pandora $TCNO_2$ retrievals for the *i*th observation, respectively, and N is the number of coincident observations.

For all comparisons, coincidence criteria were applied. For the comparisons between satellite and surface-based retrievals, at each Pandora location we used the TROPOMI pixel in which the Pandora spectrometer was located during the time of the satellite overpass (according to the TROPOMI pixel corners). The mean Pandora $TCNO_2$ was calculated within 30 min of the Sentinel-5P overpass. For Pandora and airborne coincidences, Pandora $TCNO_2$ measurements were compared to the average airborne $TCNO_2$ within a 750 m radius of the Pandora site and the temporally closest Pandora measurement following Judd et al. (2019). Sensitivity to these results can be found in Table S1 in Judd et al. (2020) and are based on minimizing the impact of large changes in short period of time as well as the benefit of averaging multiple pixels within the area to increase signal to noise and increase data volume in the presence of broken clouds. Differences in temporal criteria for Pandora comparisons to TROPOMI and airborne data are to align more with the higher spatial resolution data of the latter which can be influenced at time scales as quick as minutes (Judd et al., 2019).

3. Results and discussion

3.1. Pandora and TROPOMI $TCNO_2$ comparisons

Satellite TROPOMI $TCNO_2$ retrievals were compared with Pandora measurements over both the terrestrial and aquatic landscapes along this coastal environment (Fig. 2a). Results showed very good correlation at most sites, both over land and water (*r* of 0.87, $N = 100$). Good agreement was found between TROPOMI and Pandora in the NY urban core, where $TCNO_2$ typically shows the strongest gradients (*r* of 0.95 and 0.86, and MPD of −4% and 4%, for the Manhattan and Queens locations, respectively). Strong correlation (*r* of 0.97) was also found between satellite and shipboard Pandora retrievals over the highly dynamic NY Harbor waters. A smaller data range at New Haven, Westport, and Long Island Sound, resulted in lower correlation between TROPOMI and Pandora.

Overall, TROPOMI underestimated $TCNO_2$ relative to the surface measurements, on average by 12% across the entire region. These results are consistent with previous studies, showing that TROPOMI measurements are biased low (19–33%) compared to Pandora retrievals (Judd et al., 2020). The small change in bias is attributed to improvements made between the TROPOMI v1.3 used in Judd et al. (2020) and v2.3 retrievals within this work (van Geffen et al., 2022). TROPOMI underestimation of $TCNO_2$ was particularly pronounced over the water (MPD of −44% and − 15% in the NY Harbor and LIS, respectively). This could be at least partly explained by TROPOMI's coarser spatial resolution as well as assumptions in the NO_2 vertical profile shape and a-priori surface reflectivity (Judd et al., 2020), especially along terrestrial-aquatic interfaces characterized by highly contrasted (i.e., bright urban compared to dark water) scenes. Overall, and as discussed in more detail below, TROPOMI captured the major plumes and spatiotemporal transitions in $TCNO_2$ associated with NOx emission sources and meteorology during LISTOS (Fig. S1). Yet, it missed some of the fine spatial features and transient peaks in air pollution observed by the Pandora network across this highly dynamic urban coastal environment.

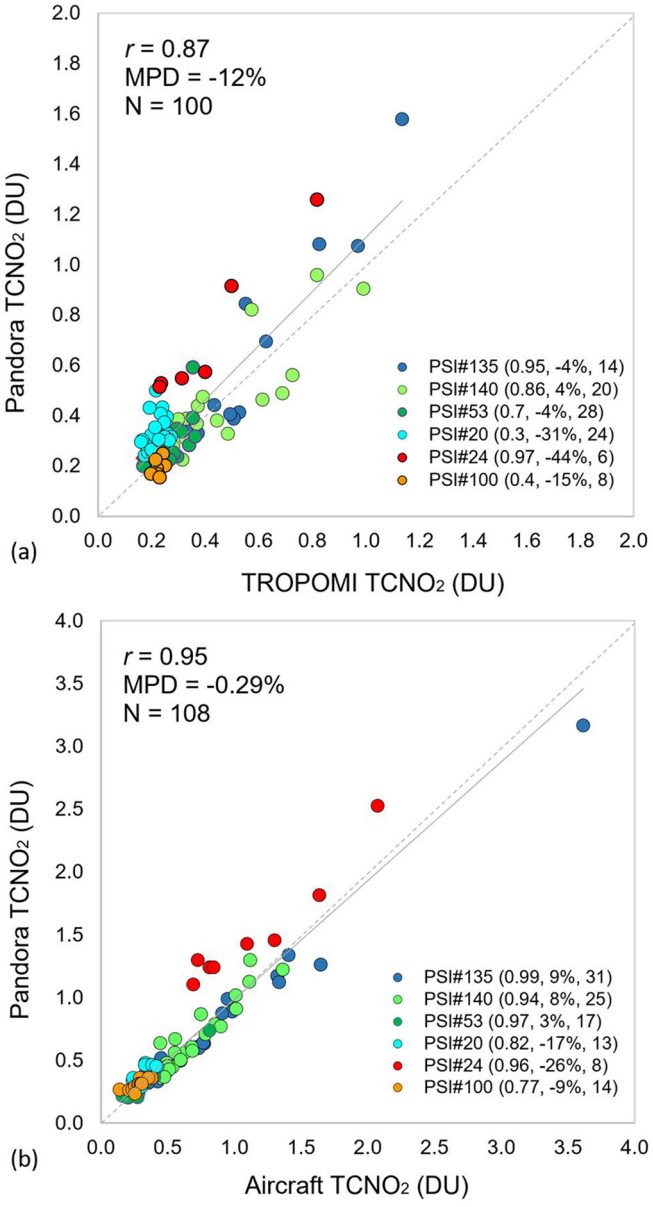

Fig. 2. (a) Comparison between TROPOMI and Pandora $TCNO_2$ at the fixed ground-based locations in NY (PSI#135, PSI#140) and CT (PSI#53, PSI#20), and over the water in NY Harbor (PSI#24) and LIS (PSI#100). (b) Comparison between aircraft and Pandora $TCNO_2$ at same locations. (Parameters *r*, MPD and N are reported for the full dataset, and for each location in the legend. The 1:1 line is indicated with the dashed line.)

3.2. Pandora and aircraft $TCNO_2$ comparisons

Airborne total NO_2 columns showed remarkably good correlation with surface Pandora retrievals, both over land and over the water ($r = 0.95$, $N = 108$, MPD < 1%; Fig. 2b). Close agreement was found in the NY urban core with aircraft slightly overestimating $TCNO_2$ compared to Pandora (*r* of 0.99 and 0.94, and MPD of 9% and 8%, for the Manhattan and

Queens locations, respectively). Multiple observations per day, from both platforms, highlighted the strong temporal dynamics in $TCNO_2$ in this urban region. As an example, both Pandora and GCAS measured a local peak of >3.0 DU in $TCNO_2$ over Manhattan in the morning of July 2, 2018, and the transition to approximately 1 DU in the afternoon (Fig. 3). Lower $TCNO_2$ was measured throughout the day by both instruments at Queens and New Haven. On July 20 and August 24, GCAS retrievals over Manhattan and Queens captured the early morning increase in $TCNO_2$, in close agreement with the Pandoras. While the aircraft did not overfly the two sites, therefore appear to miss the peaks observed by Pandora, from 15:00–16:00 UTC, these increases were apparent from the mapping perspective of the aircraft (e.g., Fig. 10). Total NO_2 columns were also highly correlated at the more rural sites of Westport and New Haven, CT (r of 0.97 and 0.82, and MPD of 3% and − 17%, respectively). $TCNO_2$ showed little temporal variability along the CT shoreline and in most cases remained <0.5 DU on the days of aircraft flights, except for September 6 when both aircraft and Pandora observed a decline in $TCNO_2$ by a factor of 3, from 0.75 DU in the morning to 0.25 DU in the afternoon, over Westport (Fig. 3). Almost 90% of the aircraft-Pandora matchups over this urban landscape, fell within ±25% difference in $TCNO_2$.

Aircraft and Pandora measurements were also strongly correlated over the water, exhibiting consistent spatiotemporal gradients in NO_2 pollution

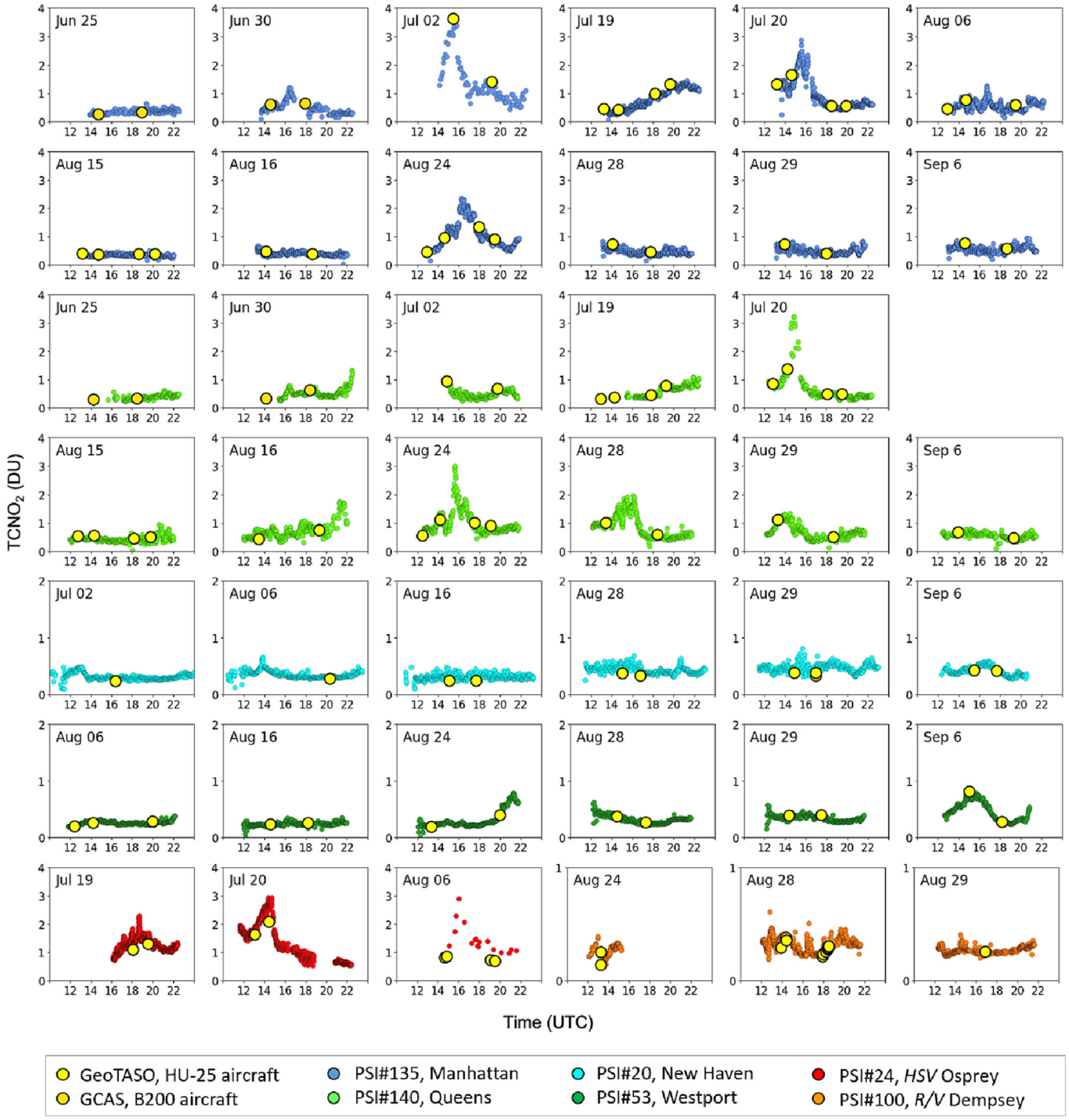

Fig. 3. Diurnal variability in $TCNO_2$ as captured by aircraft instruments (GeoTASO and GCAS), ground based Pandoras (PSI#135, #140, #20 and #53) and shipborne Pandoras (PSI#24 and #100) across the NYC-LIS land-water continuum.

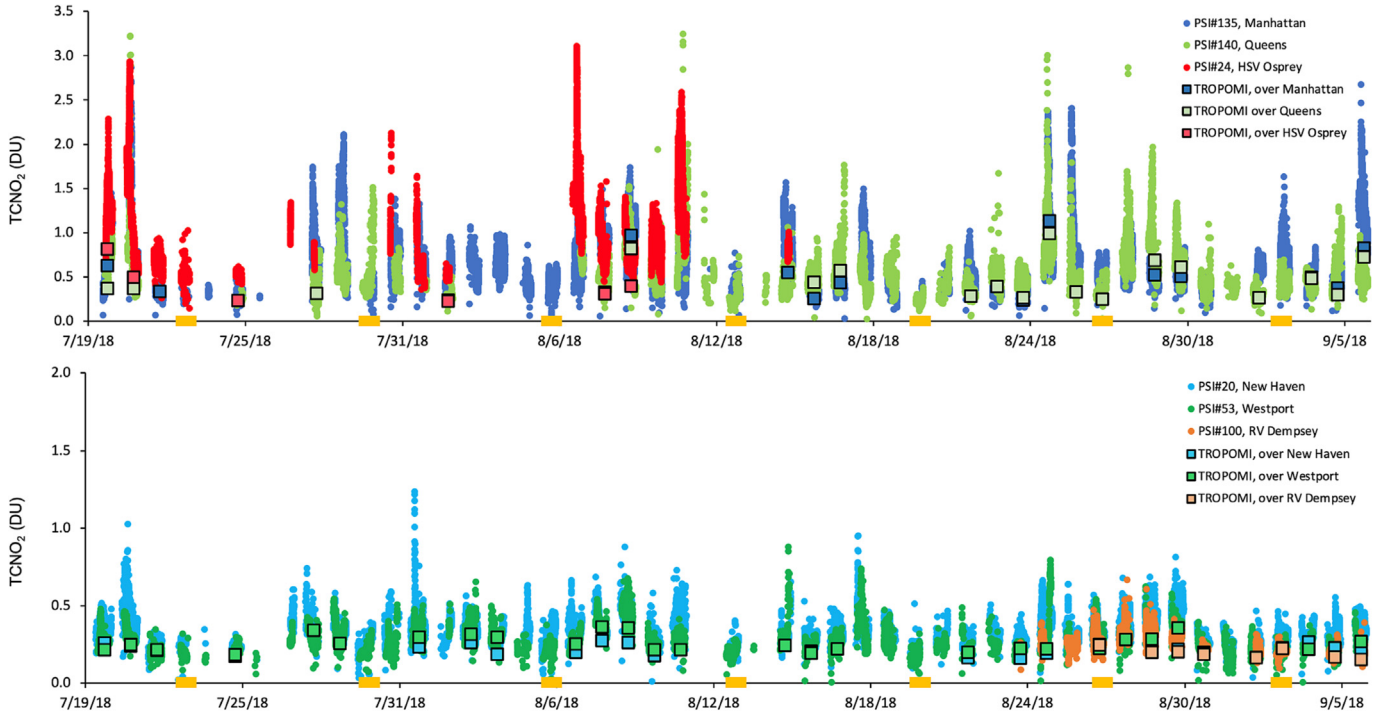

Fig. 4. Temporal variability in $TCNO_2$ as captured by TROPOMI and Pandoras over NYC, NY Harbor, and Western LIS (upper panel), and over the CT shoreline and LIS (lower panel). Sundays are indicated by orange markers on x-axis.

both over the highly heterogeneous and more polluted NY Harbor and Western LIS (sampled with PSI#24, $r = 0.96$, $N = 8$) as well as in Central and Eastern LIS where air quality conditions are typically considerably improved (sampled with PSI#100, $r = 0.77$, $N = 14$; Fig. 2b). As in the case of satellite-based retrievals, aircraft-based retrievals overall underestimated $TCNO_2$ over the water (Figs. 2, 3), but to a lesser extent than TROPOMI (MPD of −26% and −9% in the NY Harbor and LIS, respectively), most likely due to the considerably higher spatial resolution of aircraft measurements (250 m × 250 m) and higher sensitivity to surface NO_2 pollution in comparison to the TROPOMI instrument. We speculate that low biases over PSI#24 in comparison to the other sites are likely challenges in accurately portraying surface reflectivity in the heterogeneous environment of the urban/water interface exacerbated by high pollution levels in NY Harbor. Temporal dynamics in $TCNO_2$ over the water were consistent between Pandora and aircraft retrievals (Fig. 3). Both GCAS and PSI#24 captured an increase in $TCNO_2$ by approx. 0.5 DU from 13:00 UTC to 14:30 UTC in the morning of July 20, 2018, over the East River. Although $TCNO_2$ over Long Island Sound remained <0.5 DU on the days of aircraft flights, consistent with measurements along the CT shoreline (New Haven and Westport), Pandora and aircraft observations followed each other closely, capturing small-scale meteorology-driven variability in $TCNO_2$ over the water on August 28, 2018 (Fig. 3, lower panel) (see Section 3.4).

3.3. Spatiotemporal dynamics in NO_2 over the land-water continuum

Satellite imagery from TROPOMI captured significant spatial and day-to-day variability over the New York metropolitan area during July to September 2018 (Fig. S1). High $TCNO_2$ values, reaching >0.75 DU, were typically observed over eastern New Jersey, Manhattan, and Queens, often extending over the Western and Central Long Island Sound (e.g., July 9, 10, 20, August 7, 8, 24 and 29). This region, covering eastern NJ to the inner and lower NY Harbor and the Western Long Island Sound, showed the strongest temporal variability in air quality (Fig. 1). TROPOMI-retrieved $TCNO_2$ ranged within 0.24–1.14 DU and 0.24–0.99 DU over the Manhattan and Queens Pandora locations, respectively, during LISTOS (Fig. 2(a)). Yet, it remained over a much narrower range (0.17–0.36 DU and 0.16–0.27 DU, respectively) above the coastal areas of Westport and New Haven in CT. TROPOMI-retrieved $TCNO_2$ showed significant variability over the coastal aquatic domain, ranging from 0.23 to 0.82 DU over *HSV Osprey* in the New York Harbor, with

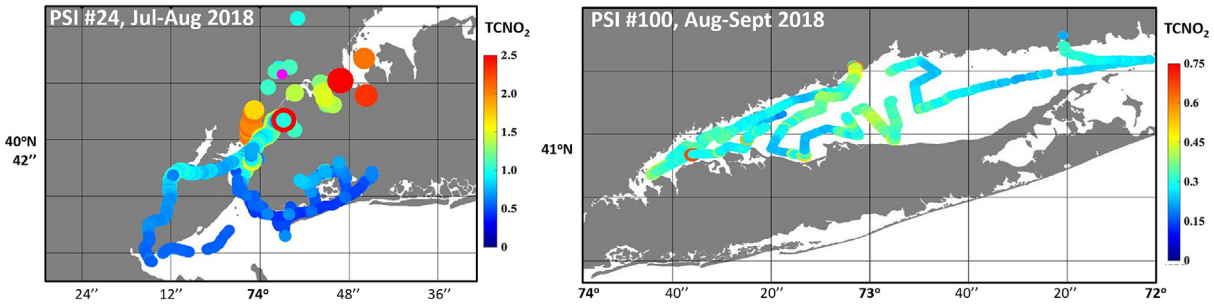

Fig. 5. Spatial distribution in $TCNO_2$ as captured by the shipboard Pandoras (left) over the New York Harbor coastal waters, Hudson River, East River, and Western Long Island Sound (PSI#24, 18 July – 14 August 2018), and (right) over the Long Island Sound waters (PSI#100, 24 August–September 5, 2018) (circle color and size scale with $TCNO_2$).

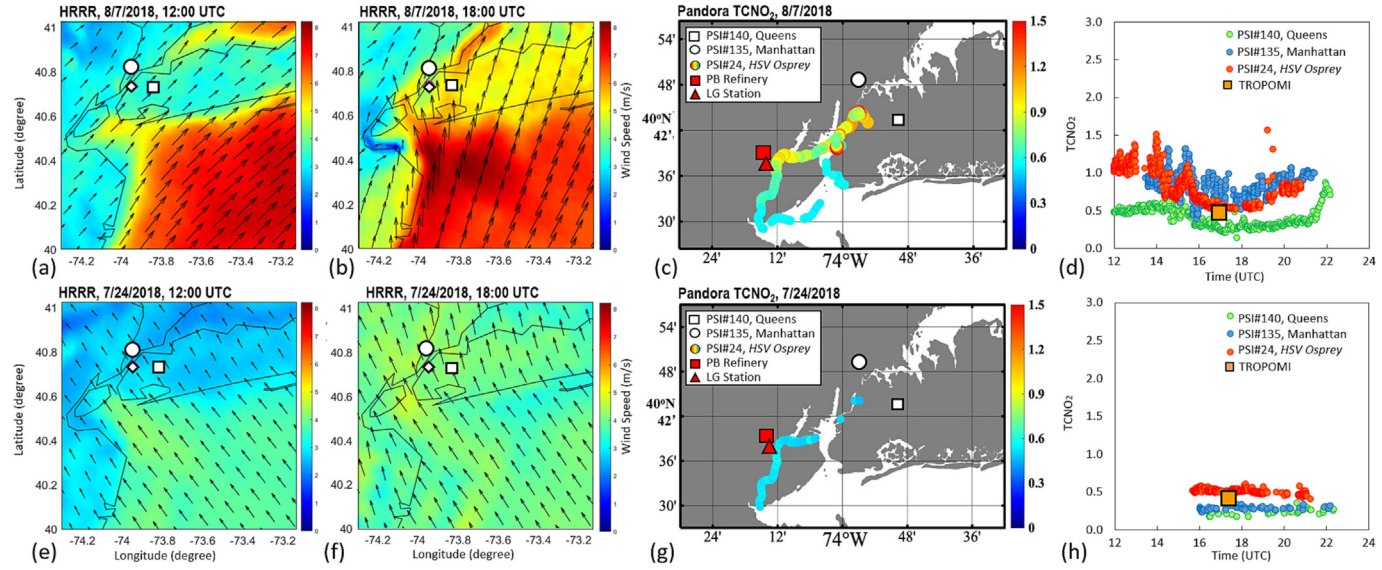

Fig. 6. HRRR winds fields at (a) 12:00 UTC and (b) 18:00 UTC on 7 August 2018. (c) PSI#24 onboard *HSV Osprey* captured strong dynamics in $TCNO_2$ over the NY Harbor, with maxima over the East River and in NW Staten Island (across PB Refinery and LG Station). (d) Temporal dynamics in Pandora-retrieved $TCNO_2$ over Queens, Manhattan, and *HSV Osprey* (TROPOMI $TCNO_2$ over *HSV Osprey* also shown). Different wind conditions on 24 July 2018 (e-f) resulted in very different $TCNO_2$ distribution both over land and water (g-h).

maximum values observed over Eastern NJ, Lower Manhattan, and NY Harbor on July 19 and 20, 2018 (Figs. S1 and 4). A similarly strong variability was captured by TROPOMI in Long Island Sound, with $TCNO_2$ varying by more than a factor of 6 from 0.15 to 1.07 DU along the *R/V Dempsey* transects, with maximum values observed in western LIS on July 9, 13, and August 6, 8 and 24 (Figs. S1, 4).

Higher resolution measurements from the aircraft sensors and the network of ground based and shipboard Pandoras were overall in good agreement with TROPOMI, but also revealed finer NO_2 variability at sub-diurnal and sub-kilometer scales driven by local emissions and meteorology (Figs. 4 and 5). Pandora-retrieved $TCNO_2$ in Manhattan, NY, was on average 0.59 (±0.32) DU during the LISTOS deployments in summer 2018, consistent with long-term, pre-COVID 19 pandemic, summertime measurements at this location (Tzortziou et al., 2022). Previous studies in NYC showed a clear seasonal cycle in $TCNO_2$ typical of Northern Hemisphere mid-latitude locations, with relatively lower values in summer and maxima occurring during the winter (Goldberg et al., 2020; Tzortziou et al., 2022). This seasonality is due largely to increased fossil fuels for domestic heating and longer tropospheric NO_2 lifetime at colder temperatures due to low light availability (van der A et al., 2008; Roberts-Semple et al., 2012;

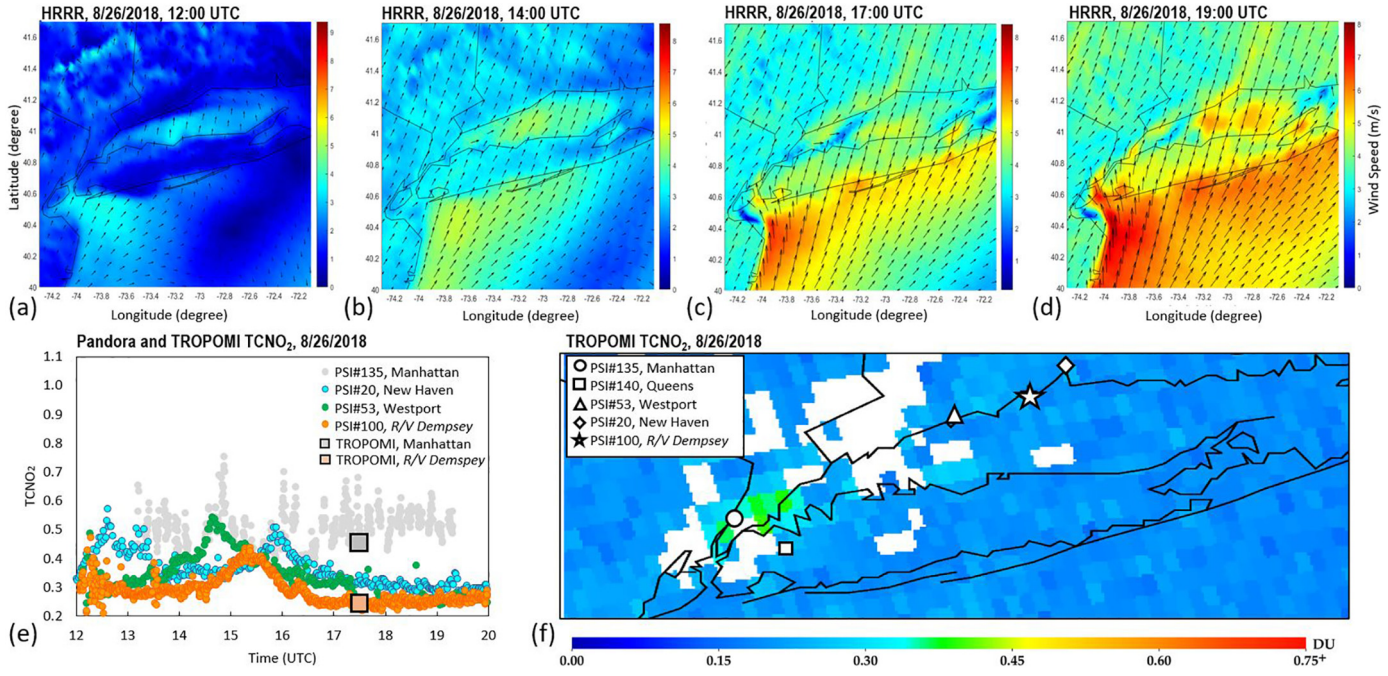

Fig. 7. (a-d) Change in wind speed and direction from 12:00 to 19:00 UTC on August 26, 2018, as estimated by the HRRR model. (e) Relatively high $TCNO_2$ (0.5–0.6 DU) was detected in the NYC core by Pandora and TROPOMI on this day, while the network of Pandoras at Westport, Milford and New Haven showed sequential peaks in $TCNO_2$ after 14:00 UTC, consistent with entrainment of polluted air mass across the CT shoreline. (f) Pandora and TROPOMI $TCNO_2$ retrievals were in excellent agreement at the time of the satellite overpass, both over the NYC urban core and over Long Island Sound.

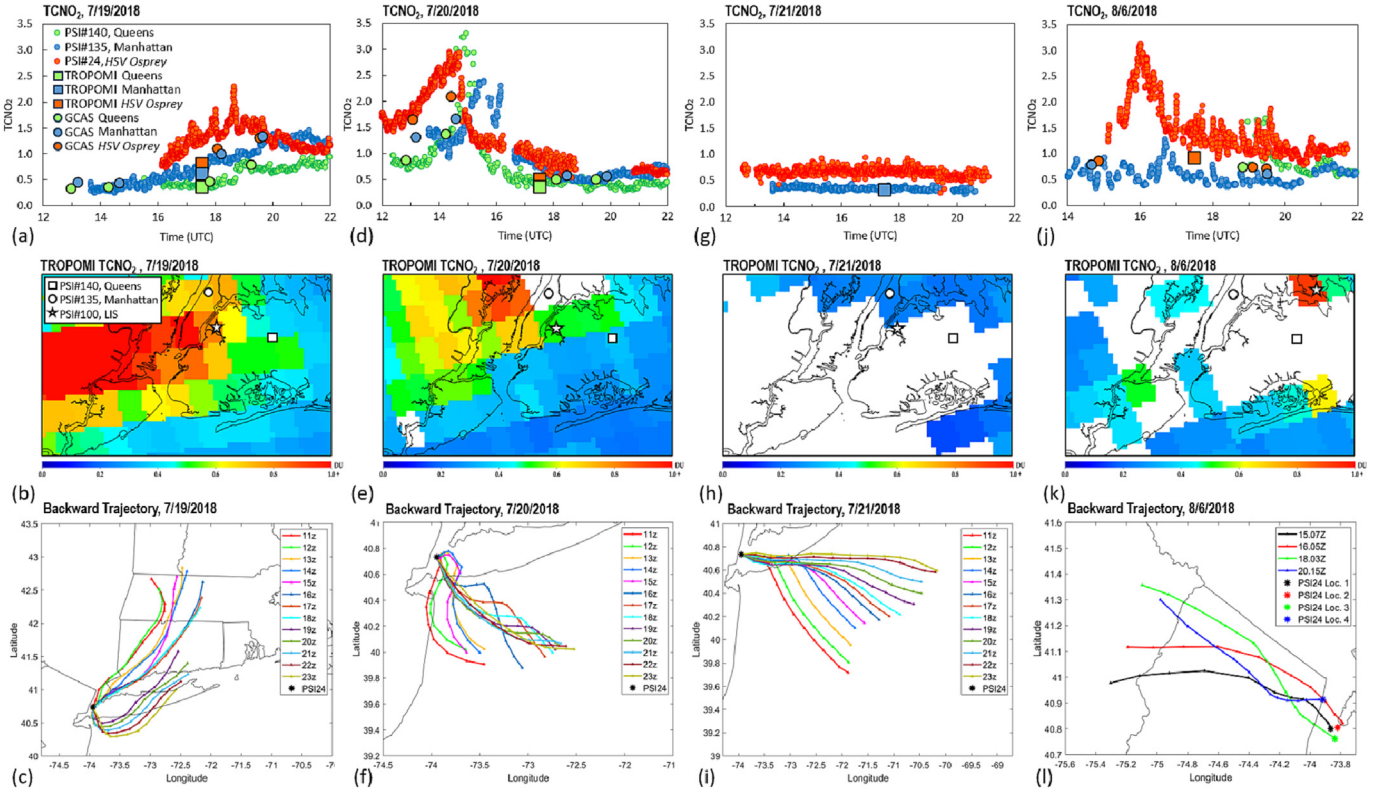

Fig. 8. Temporal and spatial dynamics in $TCNO_2$, as measured by the network of Pandoras, TROPOMI and GCAS over the NYC coastal waters and Western Sound, on 19 July 2018 (a, b) and 20 July 2018 (d, e) when sea-breeze circulations developed, 21 July 2018 (g, h) when air-quality markedly improved, and on 6 August 2018 (j, k) when another sea breeze event occurred. HYSPLIT backward trajectories, initialized at the location of *HSV Osprey* (in NY Harbor), are shown for each day (lower panel).

Tzortziou et al., 2022). Still, several cases of high NO_2 pollution were observed during the LISTOS summer. Particularly high values (often exceeding 2.0 DU) were captured by GCAS and Pandora over Manhattan on July 2, July 20, and under low wind-speed conditions (<2 ms^{-1}) on August 24, 2018 (Figs. 3, 4). Similar temporal patterns and $TCNO_2$ levels were measured by Pandora and GCAS across the East River, in Queens, NY (average Pandora $TCNO_2$ of 0.54 (±0.3) DU). NO_2 total columns along the CT shoreline, in Westport and New Haven, were overall considerably (approx. 50%) lower than measurements in New York City (0.27 DU and 0.33 DU, on average, respectively). This agrees with the spatial gradients in TROPOMI imagery (Figs. 1, S1) and previous summertime measurements along this coastal region (Tzortziou et al., 2022; Judd et al., 2020). A clear weekly cycle was captured by all Pandora instruments, with minima in $TCNO_2$ consistently measured on Sundays (Fig. 4).

In the New York Harbor, $TCNO_2$ often exceeded 2 DU, with the shipboard Pandora (PSI#24) in many cases measuring higher $TCNO_2$ than inland Pandora sites (Table 1, Fig. 4). Particularly high $TCNO_2$ levels (reaching 2 DU) were measured under relatively low wind-speed conditions (<3.5 ms^{-1}) on 30 July, as the boat transited along the Hudson River and across the PSEG Bergen Generating Station in Ridgefield, NJ (Figs. 4, 5). High $TCNO_2$ was also measured on 20 July and 6 August when *HSV Osprey* was in the East River and Western Long Island Sound, near the Astoria (AG) and Ravenswood Generating (RG) Stations in Queens, NY (Fig. 1). As discussed below, both cases were characterized by development of strong sea breeze circulations.

Another peak in $TCNO_2$ over the NY Harbor waterways, associated with local NOx emissions, was captured by PSI#24 on August 7, 2018, as *HSV Osprey* transited from the NYC-DEP Newtown Creek dock to the Bayonne Bridge and around Staten Island (Fig. 6a-d). Early in the morning (12:00 UTC) and under the influence of southwest winds (Fig. 6a), the shipboard Pandora measured $TCNO_2$ levels of approx. 1 DU over the East River and lower Manhattan with a secondary peak in $TCNO_2$ at around 15:30 UTC when *HSV Osprey* was located west of the Bayonne Bridge and across the two major NOx emission sources in Linden, NJ (i.e., Linden Generating Station (LG) and the Phillips 66 Bayway (PB) Refinery; Fig. 6c, d). As the winds changed direction under marine influence between 16:00 and 18:00 UTC (Fig. 6b), $TCNO_2$ over the water decreased to approx. 0.5 DU and remained low in the Raritan and Lower Bay areas. Although TROPOMI was in excellent agreement with the shipboard Pandora (Fig. 6d), it completely missed the spatial gradients in $TCNO_2$ in lower Manhattan and West Staten Island due to cloudy conditions over that region at the time of the satellite overpass (Fig. S1). Very different conditions were measured over the waters adjacent to the two major NJ power plants on July 24, 2018, when persistent southeast winds of marine origin kept $TCNO_2$ consistently low (< 0.5 DU) throughout the entire area (Fig. 6e-h), underlining the impact of meteorology on coastal air quality.

Transient peaks in NO_2 pollution were measured by the shipboard Pandora across Long Island Sound, with $TCNO_2$ changing by more than an order of magnitude from >2 DU in Western Narrows (6 August 2018) to <0.2 DU in Eastern Sound (29 August 2018, Figs. 4, 5). On average, NO_2 columns over the water were relatively low (0.25 DU), consistent with measurements at the two coastal CT locations (Table 1). Pandora measurements were in good agreement with satellite and aircraft retrievals, all sensors capturing very similar gradients in $TCNO_2$ over the Sound (Figs. 2-5). Beyond this spatial variability, the network of ground based and shipboard Pandoras uniquely allowed to detect rapid shifts in NO_2 pollution plumes along this coastal environment. On August 26, 2018, both TROPOMI and Pandora sensors showed relatively high $TCNO_2$ (0.5–0.7 DU) over the NYC urban core and considerably lower NO_2 levels (approx. 0.25 DU) along the CT shoreline, in excellent agreement at the time of the satellite overpass (Fig. 7e). However, the three Pandoras at Westport, New Haven, and *R/V Dempsey* (located that day at the dock in Milford, CT; Fig. 7f) also captured a peak in $TCNO_2$ of about 0.4–0.5 DU that was measured sequentially first at Westport (approx. 14:30 UTC), then at Milford (approx. 15:15 UTC), and then at New Haven (approx. 16:00 UTC; Fig. 7e). Surface winds on that morning were predominantly from southern direction,

bringing relatively clean marine air masses over the Sound (Fig. 7a). Yet, at around 14:00 UTC, HRRR showed winds changing direction to westerly over Manhattan and Western Long Island Sound (Fig. 7b). West winds prevailed across a narrow path parallel to the CT shoreline until 17:00 UTC, indicating entrainment of polluted urban air masses across the CT shoreline that was sequentially captured by the Pandora sensors. The approximately 45 min time lag in the peak NO_2 measured by the Pandoras at Westport, Milford, and New Haven, is consistent with the distance of approximately 14 km between the three locations and the model estimated wind speed of approximately 5 ms^{-1}. Dissipation of this westerly plume later in the afternoon (Fig. 7d), resulted in a decrease in $TCNO_2$ along the CT coast, as shown by both TROPOMI and the Pandora network.

3.4. Sea breeze development and impact on NO_2 dynamics across the terrestrial-aquatic interface

Sea breeze circulations greatly influenced ozone concentrations near the LIS coast during LISTOS (Zhang et al., 2020). Our HYSPLIT and HRRR model simulations showed development of 31 sea breeze events during July 18 to September 5, 2018 (days with strongest sea breeze circulations are shown in Fig. S2). The network of shipboard and ground based Pandoras, combined with satellite and aircraft data, allowed for the first time to quantify the impact of sea breezes on NO_2 dynamics over both the coastal terrestrial and aquatic domains. Such an event developed on 19 July 2018, when *HSV Osprey* was located at Newtown Creek in Greenpoint, Brooklyn (Figs. 8a-c, 10, 11). In the morning (16:00 UTC), the shipboard Pandora showed similar $TCNO_2$ levels with the PSIs at Manhattan and Queens, in good agreement with GCAS. Yet, conditions changed later that day (17:00–20:00 UTC), with both Pandoras and GCAS measuring an increase in NO_2, and higher total column amounts over the water compared to inland locations (Fig. 8a). Spatial gradients in Pandora and aircraft retrievals over Manhattan, Queens, and NY Harbor were consistent with TROPOMI at the time of the satellite overpass, showing accumulation of NO_2 over eastern New Jersey, Manhattan, and the Inner Harbor (Fig. 8b).

HRRR model simulations showed weak north winds early on that day, and development of sea breeze circulations at around 16:00 UTC (Fig. 9). A well-defined sea breeze front (indicated by the narrow zone of convergent low-speed winds in Fig. 9*)* was over the location of *HSV Osprey* at

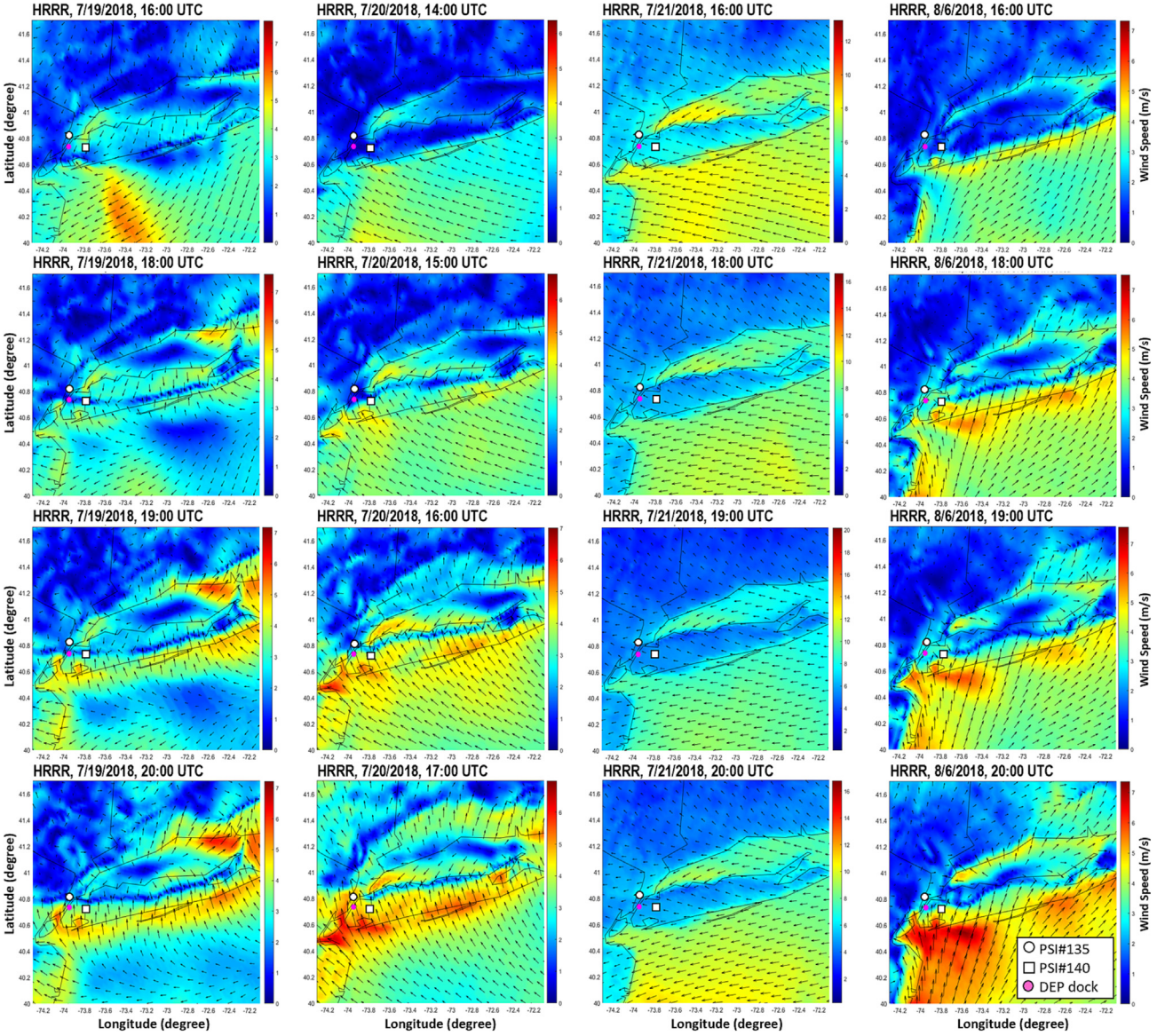

Fig. 9. Surface winds maps estimated using the HRRR model for July 19, 20, 21 and August 6, 2018. The locations of the Manhattan and Queens Pandoras, as well as the NYC DEP dock are shown. A well-defined sea breeze front was over the location of the shipboard Pandora (NYC DEP dock) at 18:00 UTC on 19 July and at 15:00 UTC on 20 July 2018. Stronger east-southeast winds persisted on 21 July 2018. Another sea breeze event occurred on August 6, 2018 (when PSI#24 was transiting in Western Long Island Sound).

18:00 UTC, consistent with the time of peak $TCNO_2$ measured by PSI#24. The front advanced inland and over the locations of the Queens Pandora at 19:00 UTC and the Manhattan Pandora at 20:00 UTC, coinciding with the maxima in $TCNO_2$ at these locations. After 20:00 UTC, higher-speed south winds dominated over the *HSV Osprey* location, resulting in a decrease in the $TCNO_2$ measured by PSI#24. Backward air-parcel trajectories, simulated by HYSPLIT at the location of *HSV Osprey* (Fig. 8c), showed consistent results, with transport of air masses from the north-northeast early in the morning, a change in the wind direction between 16:00–18:00 UTC, and transport of marine air masses from the south after 19:00 UTC. The four consecutive maps from the airborne data also pick up on this transition with the recirculation of NO_2 visible with the wind shift (Fig. 10). While NOx is continually lost through chemical reactions to form nitric acid and alkyl nitrates throughout the transport process on this day, fresh NOx emissions are also emitted into this plume within this urban area.

Stagnant conditions persisted over this area the next morning, 20 July 2018, when high $TCNO_2$ values were measured right after morning rush hour at all three Pandora locations and particularly over *HSV Osprey* (Fig. 8d). A strong temporal gradient, with $TCNO_2$ reaching >1.5 DU, was captured by the Pandoras and GCAS, but was completely missed by TROPOMI that measured much lower NO_2 consistent with the surface and aircraft instruments at the time of the satellite overpass (Fig. 8e). The time lag in maximum $TCNO_2$ measured by PSI#24, #140 and #135 was due to the movement of another sea breeze front over this area (Fig. 9). Surface wind maps showed development of a narrow convergence zone, with the sea breeze front moving over Queens at approximately 15:00 UTC and over Upper West Manhattan at 16:00 UTC, in agreement with the 1-h time lag in max $TCNO_2$ between the two locations. HYSPLIT air mass trajectories (Fig. 8f) showed development of stagnant conditions from 12:00 to 15:00 UTC, and influence from the ocean after 17:00 UTC, in agreement with the temporal variability in $TCNO_2$ measured by the shipboard Pandora (Fig. 8d). The stagnation of NO_2 over the city in the morning is clearly visible from GCAS along with advection indicated by the extension of plumes from point sources inland by late morning and continued advection of emissions throughout the afternoon (Fig. 10).

Air quality conditions markedly changed on July 21, with a transition to stronger southeast winds of marine origin that cleared the air and resulted in considerably lower $TCNO_2$ amounts across the whole area, as shown by both TROPOMI and Pandoras (Fig. 8g-h). HRRR model simulations showed stronger winds and influence from the ocean throughout the day, in agreement with HYSPLIT simulated backward trajectories (Figs. 8i, 9). The airborne instruments did not fly on this day as conditions were too cloudy.

Another sea breeze event occurred on August 6, 2018, when low winds ($< 1\ ms^{-1}$) in the morning hours and the development of a convergence zone over Long Island at 16:00 UTC (Fig. 9) resulted in strong stagnation over the Western Sound. According to previous studies (Zhang et al., 2020; Rogers et al., 2020), August 6 was characterized by a combined influence of sea breeze circulation and complicated regional ozone exceedance conditions that resulted in the state of New York issuing an Air Quality Health Alert (New York Department of Environmental Conservation, 2018). The shipboard Pandora, transiting in Western Narrows that day, measured some of the highest $TCNO_2$ levels in the region, reaching 3 DU at 16:00 UTC (Fig. 8j), compared to <1 DU at the Manhattan urban core location. Similarly, GCAS captured elevated tropospheric NO_2 columns over Western Long Island (Fig. 10). An increase in the winds as the sea breeze front moved inland coincided with lower but still elevated NO_2 over the western LIS, with both PSI#24 and TROPOMI retrieving column amounts >1 DU. The Pandora-retrieved $TCNO_2$ further decreased as *HSV Osprey* transited to the Upper NY Bay and the Hudson River later that day (Fig. 8j).

Despite the lower sun angles, a classic ozone exceedance event developed over Long Island and coastal Connecticut later in summer, on August 28, 2018 (Ma et al., 2021). The combination of satellite, aircraft, ground-based and shipboard Pandora measurements captured the different phases of this event and the distribution of NO_2 levels in the NY urban core and LIS area that likely contributed to ozone formation (Fig. 11). South winds in the morning of August 28 (14:00 UTC) converged with weak ($< 2\ ms^{-1}$)

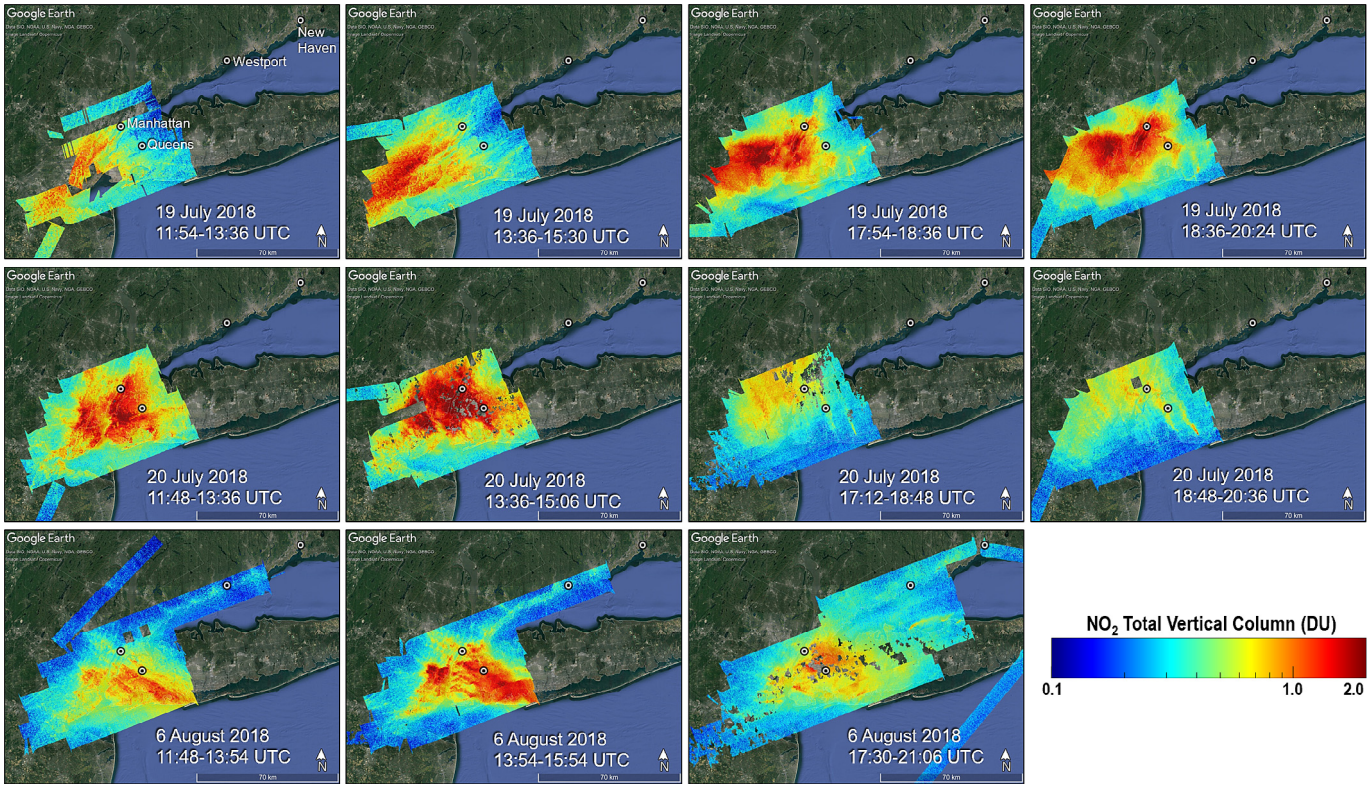

Fig. 10. Aircraft GCAS retrievals of total column $TCNO_2$ during the development of sea breeze circulations along the NY-CT shorelines, on July 19 (upper panel), July 20 (mid panel) and August 6 (lower panel) 2018. Maximum $TCNO_2$ was observed over NY Harbor during 18:36–20:24 UTC on July 19, 13:36–15:06 UTC on July 20, and 13:54–15:54 UTC on August 6, in excellent agreement with the shipboard Pandora measurements (shown in Fig. 8).

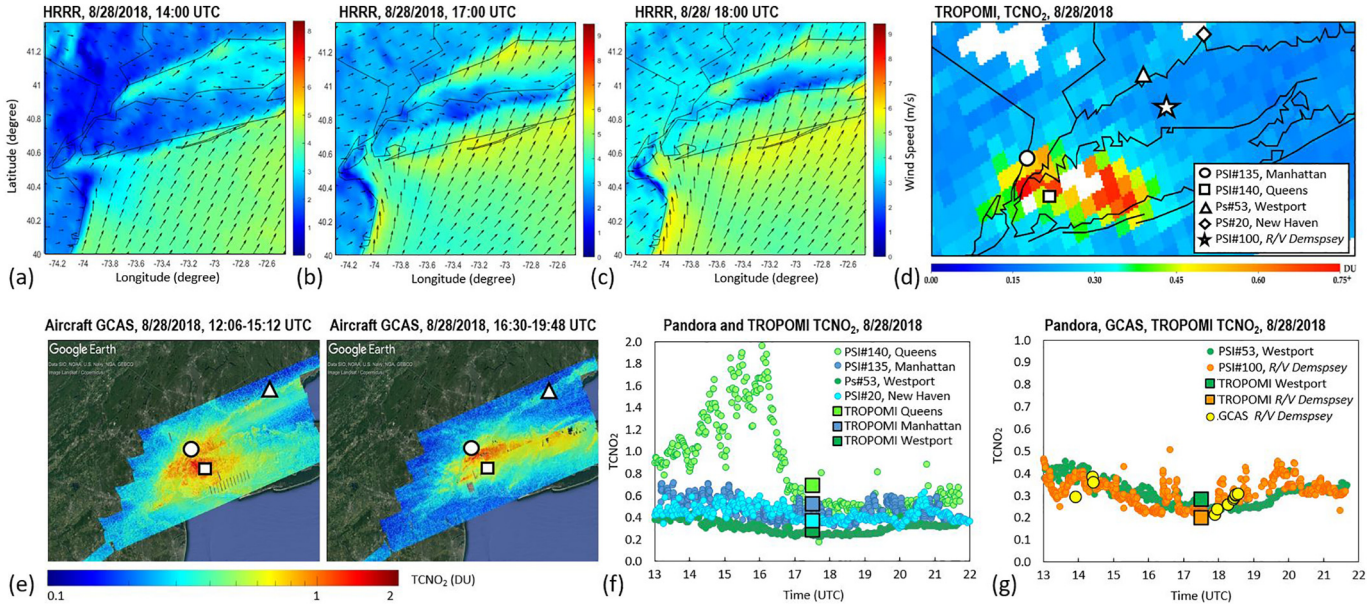

Fig. 11. (a-c) Change in wind speed and direction at 14:00, 17:00 and 18:00 UTC on August 28, 2018, from the HRRR model, showing development of stagnant conditions across Long Island and over the Sound. (d) TROPOMI $TCNO_2$ on the same day. (e) GCAS $TCNO_2$ in the morning and afternoon of August 28, 2018. (f-g) Time series of $TCNO_2$ from the ground based and shipboard Pandoras, GCAS, and TROPOMI, showing an increase in $TCNO_2$ over the Sound after 17:00 UTC (g).

surface west winds over Long Island resulting in stagnant conditions and accumulation of urban pollution especially over Western Long Island. In addition to local urban emissions, air quality over New York on that day was also influenced by long-distance transport of smoke from active fires in the southeastern United States, causing significant increases in regional concentrations of air pollutants, including particulate matter (i.e., $PM_{2.5}$), black carbon (BC), and carbon monoxide (CO) for 3 days (Rogers et al., 2020). Aircraft measurements showed elevated $TCNO_2$ over the NYC urban core with NO_2 pollution peaking over Queens, consistent with a strong increase in $TCNO_2$ levels to >1 DU at the ground-based Queens Pandora location after 14:00 UTC that reached >2 DU at 16:00 UTC (Fig. 11f). $TCNO_2$ levels remained significantly lower at the Pandora locations in Manhattan and along the CT shoreline, consistent with aircraft retrievals (Fig. 11e-f). By 17:00 UTC, the sea breeze front had progressed over the northern Long Island shoreline, reshaping the distribution of NO_2 over this coastal environment. Total NO_2 columns decreased at the Queens Pandora location to 0.6–0.7 DU, in excellent agreement with the TROPOMI overpass, while GCAS showed the NO_2 plume moving east and accumulating along the northern Long Island shore. These meteorological conditions impacted NO_2 over the Sound, resulting in high total columns (approx. 0.4 DU, compared to an average of 0.28 DU during LISTOS, Table 1) at low wind-speed conditions in the morning (13:00–14:00 UTC), both at the Westport coastal location and over *R/V Dempsey* (Fig. 11g). An increase in wind speed over the Sound around the time of the satellite overpass (17:00 UTC) coincided with a decrease in $TCNO_2$ at Westport and over the water, captured by the Pandoras, GCAS, and TROPOMI. The progression of the sea breeze convergence zone (and slower winds) over the Sound after 18:00 UTC coincided with a gradual increase in $TCNO_2$ both along the CT coastline and particularly – as shown in excellent agreement by GCAS and PSI#100 – over central Long Island Sound, resulting in higher NO_2 pollution over water than over land.

4. Summary and conclusions

Integration of model simulations, satellite retrievals, aircraft data, and measurements from a network of fixed and mobile Pandoras provided a mechanistic understanding of the strong gradients and rapid transitions in NO_2 pollution observed across the NY-LIS land-water continuum during LISTOS. Spatiotemporal gradients in satellite $TCNO_2$ retrievals were found to be highly correlated with aircraft, land-based, and shipboard observations. Yet, TROPOMI overall underestimated $TCNO_2$ and missed peaks in NO_2 pollution caused by rush hour emissions or pollution accumulation during sea breezes. With multiple observations per day, at much finer spatial resolution than TROPOMI, aircraft measurements showed very good agreement with Pandora $TCNO_2$ retrievals (r of 0.95, $N = 108$), with almost 90% of the GCAS-Pandora matchups over this urban landscape falling within ±25% difference. Stronger agreement was found between TROPOMI, aircraft, and Pandora over land, while over the aquatic domain satellite, and to a lesser extent aircraft, retrievals underestimated $TCNO_2$, both over LIS and particularly in the more optically complex and dynamic NY Harbor environment. This highlights the need for more measurements to better constrain algorithm assumptions regarding the vertical profile of NO_2 and surface reflectance, especially over highly contrasted terrestrial (bright urban) and aquatic (dark and strongly absorbing) interfaces. Datasets that combine information on NO_2 total column amounts, vertical distribution, and water properties (in-water absorption, attenuation, and water-leaving radiance) would be particularly useful for improved models and remote sensing algorithms of critical air pollutants.

In the New York metropolitan area, local NO_x emissions from major power plants and transportation resulted in typically high NO_2 conditions over eastern New Jersey, Manhattan, Queens, and the NY Harbor coastal waters. These regions were shown as air-pollution hotspots with >0.75 DU $TCNO_2$ even on the coarser satellite TROPOMI imagery. Wind direction, wind speed, and sea breeze circulations with converging surface winds and development of stagnant conditions, were the main factors driving spatial and temporal variability in NO_2 in this coastal region. A change in $TCNO_2$ by more than a factor of three (e.g., from <1 DU to >3 DU), over a period of <3 h was often measured by the coastal Pandoras during the development of almost stagnant (<1 ms^{-1} wind speed) conditions and sea breeze circulations. The network of shipboard and land-based Pandoras uniquely captured high-NO_2 plumes (> 2 DU) advancing inland over this terrestrial-aquatic interface, coincident with the slow inland movement of the sea breeze front. Transition to stronger southeast winds of marine origin typically cleared the air, in some cases within a few hours, and resulted in lower $TCNO_2$ amounts across the whole area, shown by shipboard and ground-based Pandoras, aircraft and satellite imagery.

NO_2 pollution plumes from the NJ/NYC urban core often extended >30 km over the Western and Central Long Island Sound. In one of the

cases highlighted in this study, westerly winds prevailed across a narrow path parallel to the CT coastline, enhancing the entrainment of polluted urban air masses along the northern Long Island Sound that was sequentially captured by the network of Pandora instruments in Westport, Milford, and New Haven. Sea breeze circulations exacerbated air pollution in NY Harbor but - maybe more surprising - also impacted NO_2 dynamics over the typically less polluted Sound. One such case was captured in late August 2018 when coincident aircraft and shipboard measurements showed, in excellent agreement, an increase in $TCNO_2$ as a sea breeze front moved over the Sound resulting in higher NO_2 columns over water than over land. Driven by such meteorological conditions and urban pollution transport to downwind areas, column NO_2 in Long Island Sound during LISTOS varied by more than an order of magnitude, from 0.2 DU to 2 DU. Maxima in $TCNO_2$ typically occurred in Western LIS. Such high NO_2 levels could have significant impacts, through dry and wet atmospheric deposition, on the vulnerable aquatic ecosystem in Western Narrows that is already experiencing high nutrient loads, seasonal summer hypoxia, and recurrent harmful algal blooms (Luo et al., 2002). Transport of high NO_2 pollution has also significant implications for the health of diverse communities that live and work along this urban coastline. Long Island is characterized by stark disparities at the zip-code level, with a large population facing significant problems related to pollution, poverty, and access to health care (Lambert, 2002). Air quality issues in this area, thus, can have major impacts on the health of such underserved communities and vulnerable (e.g., elderly) populations.

About 6% (or, 23.3 million people) of the US population lives within a 50-mile radius of Long Island Sound (U.S. Census Bureau, 2021). Capturing transitions in NO_2 pollution and understanding the impacts of both human activity as well as meteorology on NO_2 dynamics along this economically and ecologically important coastline is critical, especially given its increasing vulnerability to climate change stressors. Sea breezes are commonly observed along the Eastern US coastline. During the LISTOS summer, HRRR captured 14 sea breezes. The combination of measurements from shipboard, ground-based, aircraft, and satellite platforms in this study provided an unprecedented spatiotemporal coverage of the impact of these transient meteorological conditions on NO_2 pollution across this highly dynamic urban land-water continuum. The frequency and severity of sea breeze circulations are projected to increase with coastal urbanization and climate change, and such events are expected to be more prevalent in the future starting earlier in the spring and ending later in the fall (Leung and Gustafson, 2005; Zhang et al., 2009; Horton et al., 2012). Increases in NOx emissions, associated with increased demand for air-conditioning on hot days under warming climate conditions, are also expected to result in higher concentrations of NO_2, exacerbating coastal air pollution (He et al., 2014). Results from this study have, thus, important implications for air quality management, both for improving understanding of ozone chemistry and pollutant transport from urban NO_x emission hot spots to downwind terrestrial and aquatic ecosystems, as well as for assessing exposure to NO_2 pollution and impacts on human health in a changing climate.

Supplementary data to this article can be found online at https://doi.org/10.1016/j.scitotenv.2023.165144.

CRediT authorship contribution statement

MT designed the study, collected and analyzed the field datasets, contributed to the satellite data analysis, and wrote the paper with input from the co-authors; CPL and DN provided the HYSPLIT and HRRR model output; DLG processed the TROPOMI satellite data; LJ processed the aircraft data; TL, DN and CFK contributed to the field and satellite data processing and analysis; AC and NA contributed to the Pandora data collection and processing. All co-authors reviewed and edited the paper for clarity.

Data availability

All Pandora data used in this study can be downloaded freely from the Pandonia Global Network website https://www.pandonia-global-network.org/. Our gridded satellite NO_2 products and output from our model can be made available upon request. Airborne data are publicly available at the NASA Airborne Sciences Data Center: DOI:https://doi.org/10.5067/SUBORBITAL/LISTOS/DATA001

Declaration of competing interest

The authors declare that they have no known competing financial interests or personal relationships that could have appeared to influence the work reported in this paper.

Acknowledgements

We thank Thomas Hanisco, Moritz Mueller, and the NASA Pandora Project and ESA Pandonia Project staff for assistance in the field and for establishing the Pandora sites used in this investigation. We thank Lukas Valin, Jim Szykman and the EPA Air, Climate, and Energy research program and Center for Environmental Measurements and Modeling for operating and maintaining the EPA Pandora sites used in this investigation. We also thank NYC DEP and CT-DEEP, including Beau Ranheim and Matt Lyman and the crews of the *HSV Osprey* and *R/V Dempsey* for their assistance in the deployment of the shipboard Pandora instruments. This research was supported by NASA Applied Science Program, grant number NNX16AD60G, NASA Interdisciplinary Science (IDS) Program, grant 80NSSC17K0258, and NOAA Earth System Sciences and Remote Sensing Technologies award NA16SEC4810008.

References

van der A, R.J., Eskes, H.J., Boersma, K.F., van Noije, T.P.C., Roozendael, M.V., Smedt, I.D., Peters, D.H.M.U., Meijer, E.W., 2008. Trends, seasonal variability and dominant NOx source derived from a ten year record of NO2 measured from space. J. Geophys. Res. Atmos. 113. https://doi.org/10.1029/2007JD009021.

Alexander, C., 2021. The High-Resolution Rapid Refresh Model (HRRR). Global Systems Laboratory, National Oceanic and Atmospheric Administration accessed 15 July 2022 https://rapidrefresh.noaa.gov/hrrr/.

Beirle, S., Platt, U., Wenig, M., Wagner, T., 2003. Weekly cycle of NO_2 by GOME measurements: a signature of anthropogenic sources. Atmos. Chem. Phys. 3, 2225–2232. https://doi.org/10.5194/acp-3-2225-2003.

Beirle, S., Borger, C., Dörner, S., Li, A., Hu, Z., Liu, F., Wang, Y., Wagner, T., 2019. Pinpointing nitrogen oxide emissions from space. Sci. Adv. 5, eaax9800. https://doi.org/10.1126/sciadv.aax9800.

Boersma, K.F., Eskes, H.J., Richter, A., De Smedt, I., Lorente, A., Beirle, S., van Geffen, J.H.G.M., Zara, M., Peters, E., Van Roozendael, M., Wagner, T., Maasakkers, J.D., van der A, R.J., Nightingale, J., De Rudder, A., Irie, H., Pinardi, G., Lambert, J.-C., Compernolle, S.C., 2018. Improving algorithms and uncertainty estimates for satellite NO_2 retrievals: results from the quality assurance for the essential climate variables (QA4ECV) project. Atmos. Meas. Tech. 11, 6651–6678. https://doi.org/10.5194/amt-11-6651-2018.

Burnett, R.T., Stieb, D., Brook, J.R., Cakmak, S., Dales, R., Raizenne, M., Vincent, R., Dann, T., 2004. Associations between short-term changes in nitrogen dioxide and mortality in Canadian cities. Arch. Environ. Health 59, 228–236. https://doi.org/10.3200/AEOH.59.5.228-236.

Burns, D.A., Bhatt, G., Linker, L.C., Bash, J.O., Capel, P.D., Shenk, G.W., 2021. Atmospheric nitrogen deposition in the Chesapeake Bay watershed: a history of change. Atmos. Environ. 251, 118277.

Celarier, E.A., Brinksma, E.J., Gleason, J.F., Veefkind, J.P., Cede, A., Herman, J.R., Ionov, D., Goutail, F., Pommereau, J.P., Lambert, J.C., Van Roozendael, M., 2008. Validation of ozone monitoring instrument nitrogen dioxide columns. J. Geophys. Res. Atmos. 113 (D15).

Chi, Y., Fan, M., Zhao, C., Sun, L., Yang, Y., Yang, X., Tao, J., 2021. Ground-level NO_2 concentration estimation based on OMI tropospheric NO2 and its spatiotemporal characteristics in typical regions of China. Atmos. Res. 264, 105821.

Choi, S., Lamsal, L.N., Follette-Cook, M., Joiner, J., Krotkov, N.A., Swartz, W.H., Pickering, K.E., Loughner, C.P., Appel, W., Pfister, G., Saide, P.E., Cohen, R.C., Weinheimer, A.J., Herman, J.R., 2020. Assessment of NO2 observations during DISCOVER-AQ and KORUS-AQ field campaigns. Atmos. Meas. Tech. 13, 2523–2546. https://doi.org/10.5194/amt-13-2523-2020.

Clark, L.P., Millet, D.B., Marshall, J.D., 2014. National patterns in environmental injustice and inequality: outdoor NO2 air pollution in the United States. PLoS One 9 (4), e94431.

Clean Air Interstate Rule, CAIR, 2009. Environmental Protection Agency (EPA), 40 CFR Part 52 [EPA–R03–OAR–2009–0370; FRL–9090–2]. https://www.govinfo.gov/content/pkg/FR-2009-12-10/pdf/E9-29216.pdf.

Colle, B.A., Novak, D.R., 2010. The New York bight jet: climatology and dynamical evolution. Mon. Weather Rev. 138 (6), 2385–2404.

Couillard, M.H., Schwab, M.J., Schwab, J.J., Lu, C.-H.(.S.)., Joseph, E., Stutsrim, B., et al., 2021. Vertical profiles of ozone concentrations in the lower troposphere downwind of

New York City during LISTOS 2018–2019. J. Geophys. Res. Atmos. 126, e2021JD035108. https://doi.org/10.1029/2021JD035108.
Crutzen, Paul J., 1979. The role of NO and NO2 in the chemistry of the troposphere and stratosphere. Annu. Rev. Earth Planet. Sci. 7.1, 443–472.
Decina, S.M., Templer, P.H., Hutyra, L.R., Gately, C.K., Rao, P., 2017. Variability, drivers, and effects of atmospheric nitrogen inputs across an urban area: emerging patterns among human activities, the atmosphere, and soils. Sci. Total Environ. 609, 1524–1534. https://doi.org/10.1016/j.scitotenv.2017.07.166.
Decina, S.M., Hutyra, L.R., Templer, P.H., 2020. Hotspots of nitrogen deposition in the world's urban areas: a global data synthesis. J. Ecol. Environ. 18, 92–100. https://doi.org/10.1002/fee.2143.
Di Bernardino, A., Iannarelli, A.M., Casadio, S., Mevi, G., Campanelli, M., Casasanta, G., Cede, A., Tiefengraber, M., Siani, A.M., Spinei, E., Cacciani, M., 2021. On the effect of sea breeze regime on aerosols and gases properties in the urban area of Rome, Italy. Urban Climate 37, 100842.
Dix, B., de Bruin, J., Roosenbrand, E., Vlemmix, T., Francoeur, C., Gorchov-Negron, A., McDonald, B., Zhizhin, M., Elvidge, C., Veefkind, P., Levelt, P., de Gouw, J., 2020. Nitrogen oxide emissions from U.S. oil and gas production: recent trends and source attribution. Geophys. Res. Lett. 47, e2019GL085866. https://doi.org/10.1029/2019GL085866.
Duan, Y., Liao, Y., Li, H., Yan, S., Zhao, Z., Yu, S., Fu, Y., Wang, Z., Yin, P., Cheng, J., Jiang, H., 2019. Effect of changes in season and temperature on cardiovascular mortality associated with nitrogen dioxide air pollution in Shenzhen, China. Sci. Total Environ. 697, 134051. https://doi.org/10.1016/j.scitotenv.2019.134051.
Duncan, B.N., Lamsal, L.N., Thompson, A.M., Yoshida, Y., Lu, Z., Streets, D.G., Hurwitz, M.M., Pickering, K.E., 2016. A space-based, high-resolution view of notable changes in urban NOx pollution around the world (2005–2014). J. Geophys. Res. Atmos. 121, 976–996. https://doi.org/10.1002/2015JD024121.
Gaza, R.S., 1998. Mesoscale meteorology and high ozone in the Northeast United States. J. Appl. Meteorol. Climatol. 37 (9), 961–977.
van Geffen, J., Eskes, H., Compernolle, S., Pinardi, G., Verhoelst, T., Lambert, J.-C., Sneep, M., ter Linden, M., Ludewig, A., Boersma, K.F., Veefkind, J.P., 2022. Sentinel-5P TROPOMI NO2 retrieval: impact of version v2.2 improvements and comparisons with OMI and ground-based data. Atmos. Meas. Tech. 15, 2037–2060. https://doi.org/10.5194/amt-15-2037-2022.
Goldberg, D.L., Loughner, C.P., Tzortziou, M., Stehr, J.W., Pickering, K.E., Marufu, L.T., Dickerson, R.R., 2014. Higher surface ozone concentrations over the Chesapeake Bay than over the adjacent land: observations and models from the DISCOVER-AQ and CBODAQ campaigns. Atmos. Environ. 84, 9–19.
Goldberg, D.L., Lu, Z., Oda, T., Lamsal, L.N., Liu, F., Griffin, D., et al., 2019a. Exploiting OMI NO2 satellite observations to infer fossil-fuel CO2emissions from U.S. megacities. Sci. Total Environ. 695. https://doi.org/10.1016/j.scitotenv.2019.133805.
Goldberg, D.L., Lu, Z., Streets, D.G., de Foy, B., Griffin, D., McLinden, C.A., Lamsal, L.N., Krotkov, N.A., Eskes, H., 2019b. Enhanced capabilities of TROPOMI NO2: estimating NOX from North American cities and power plants. Environ. Sci. Technol. 53, 12594–12601. https://doi.org/10.1021/acs.est.9b04488.
Goldberg, D.L., Anenberg, S.C., Griffin, D., McLinden, C.A., Lu, Z., Streets, D.G., 2020. Disentangling the impact of the COVID-19 lockdowns on urban NO_2 from natural variability. Geophys. Res. Lett. 47 (17) (p.e2020GL089269).
Goldberg, D.L., Anenberg, S.C., Lu, Z., Streets, D.G., Lamsal, L.N., McDuffie, E., E., Smith, S.J., 2021. Urban NOx emissions around the world declined faster than anticipated between 2005 and 2019. Environ. Res. Lett. 16 (11), 115004. https://doi.org/10.1088/1748-9326/ac2c34.
Griffin, D., Zhao, X., McLinden, C. A., Boersma, F., Bourassa, A., Dammers, E., Degenstein, D., Eskes, H., Fehr, L., Fioletov, V., Hayden, K., Kharol, S. K., Li, S.-M., Makar, P., Martin, R. V., Mihele, C., Mittermeier, R. L., Krotkov, N., Sneep, M., Lamsal, L. N., Linden, M. ter, Geffen, J. van, Veefkind, P., and Wolde, M., 2019. High-resolution mapping of nitrogen dioxide with TROPOMI: first results and validation over the Canadian oil sands, Geophys. Res. Lett., 46, 1049–1060, doi: https://doi.org/10.1029/2018GL081095.
Gu, B., Zhu, Y., Chang, J., Peng, C., Liu, D., Min, Y., Luo, W., Howarth, R.W., Ge, Y., 2011. The role of technology and policy in mitigating regional nitrogen pollution. Environ. Res. Lett. 6, 014011.
He, H., C. P. Loughner, J. W. Stehr, H. L. Arkinson, L. C. Brent, M. B. Follette-Cook, M. A. Tzortziou, K. E. Pickering, A. M. Thompson, D. K. Martins, G. S. Diskin, B. E. Anderson, J. H. Crawford, A. J. Weinheimer, P. Lee, J. C. Hains, and R. R. Dickerson. 2014. An elevated reservoir of air pollutants over the Mid-Atlantic States during the 2011 DISCOVER-AQ campaign: Airborne measurements and numerical simulations, Atmos. Environ., 85, 18–30, 2014.
Herman, J., Spinei, E., Fried, A., Kim, J., Kim, J., Kim, W., Cede, A., Abuhassan, N., Segal-Rozenhaimer, M., 2018. NO_2 and HCHO measurements in Korea from 2012 to 2016 from Pandora spectrometer instruments compared with OMI retrievals and with aircraft measurements during the KORUS-AQ campaign. Atmos. Meas. Tech. 11, 4583–4603. https://doi.org/10.5194/amt-11-4583-2018.
Herman, J., Abuhassan, N., Kim, J., Kim, J., Dubey, M., Raponi, M., Tzortziou, M., 2019. Underestimation of column NO_2 amounts from the OMI satellite compared to diurnally varying ground-based retrievals from multiple PANDORA spectrometer instruments. Atmos. Meas. Tech. 12, 5593–5612. https://doi.org/10.5194/amt-12-5593-2019.
Horton, D.E., Harshvardhan, Diffenbaugh, N.S., 2012. Response of air stagnation frequency to anthropogenically enhanced radiative forcing. Environ. Res. Lett. 7, 044034. https://doi.org/10.1088/1748-9326/7/4/044034.
Ialongo, I., Virta, H., Eskes, H., Hovila, J., Douros, J., 2020. Comparison of TROPOMI/Sentinel-5 precursor NO_2 observations with ground-based measurements in Helsinki. Atmos. Meas. Tech. 13, 205–218. https://doi.org/10.5194/amt-13-205-2020.
Judd, L.M., Al-Saadi, J.A., Janz, S.J., Kowalewski, M.G., Pierce, R.B., Szykman, J.J., Valin, L.C., Swap, R., Cede, A., Mueller, M., Tiefengraber, M., Abuhassan, N., Williams, D., 2019. Evaluating the impact of spatial resolution on tropospheric NO2 column comparisons within urban areas using high-resolution airborne data. Atmos. Meas. Tech. 12, 6091–6111. https://doi.org/10.5194/amt-12-6091-2019.
Judd, L.M., Al-Saadi, J.A., Szykman, J.J., Valin, L.C., Janz, S.J., Kowalewski, M.G., Eskes, H.J., Veefkind, J.P., Cede, A., Mueller, M., Gebetsberger, M., Swap, R., Pierce, R.B., Nowlan, C.R., Abad, G.G., Nehrir, A., Williams, D., 2020. Evaluating sentinel-5P TROPOMI tropospheric NO_2 column densities with airborne and Pandora spectrometers near New York City and Long Island Sound. Atmos. Meas. Tech. 13, 6113–6140. https://doi.org/10.5194/amt-13-6113-2020.
Kanakidou, M., Mihalopoulos, N., Kindap, T., Im, U., Vrekoussis, M., Gerasopoulos, E., Dermitzaki, E., Unal, A., Koçak, M., Markakis, K., Melas, D., 2011. Megacities as hot spots of air pollution in the East Mediterranean. Atmos. Environ. 45 (6), 1223–1235.
Karambelas, A., 2020. LISTOS: Toward a Better Understanding of New York City's Ozone Pollution Problem, The Magazine for Environmental Managers.
Kaynak, B., Hu, Y., Martin, R.V., Sioris, C.E., Russell, A.G., 2009. Comparison of weekly cycle of NO2 satellite retrievals and NOx emission inventories for the continental United States. J. Geophys. Res. Atmos. 114. https://doi.org/10.1029/2008JD010714.
Kowalewski, M.G., Janz, S.J., 2014. Remote sensing capabilities of the GEO-CAPE airborne simulator. SPIE Conference Proceedings, San Diego, California, United States https://doi.org/10.1117/12.2062058.
Krotkov, N.A., McLinden, C.A., Li, C., Lamsal, L.N., Celarier, E.A., Marchenko, S.V., Swartz, W.H., Bucsela, E.J., Joiner, J., Duncan, B.N., Boersma, K.F., Veefkind, J.P., Levelt, P.F., Fioletov, V.E., Dickerson, R.R., He, H., Lu, Z., Streets, D.G., 2016. Aura OMI observations of regional SO_2 and NO_2 pollution changes from 2005 to 2015. Atmos. Chem. Phys. 16, 4605–4629. https://doi.org/10.5194/acp-16-4605-2016.
Lambert, B., 2002. Study calls Long Island most segregated suburb. New York Times. 5.
Leitch, J.W., Delker, T., Good, W., Ruppert, L., Murcray, F., Chance, K., Liu, X., Nowlan, C., Janz, S.J., Krotkov, N.A., Pickering, K.E., Kowalewski, M., Wang, J., 2014. The GeoTASO airborne spectrometer project. In: Butler, J.J., Xiong, X. (Jack), Gu, X. (Eds.), SPIE Proceedings. Vol. 921, p. 92181H. https://doi.org/10.1117/12.2063763?SSO=1.
Leung, L.R., Gustafson, W.I., 2005. Potential regional climate change and implications to US air quality. Geophys. Res. Lett. 32, L16711. https://doi.org/10.1029/2005GL022911.
Lorente, A., Folkert Boersma, K., Yu, H., Dörner, S., Hilboll, A., Richter, A., Liu, M., Lamsal, L.N., Barkley, M., De Smedt, I., Van Roozendael, M., Wang, Y., Wagner, T., Beirle, S., Lin, J.-T., Krotkov, N., Stammes, P., Wang, P., Eskes, H.J., Krol, M., 2017. Structural uncertainty in air mass factor calculation for NO2 and HCHO satellite retrievals. Atmos. Meas. Tech. 10, 759–782. https://doi.org/10.5194/amt-10-759-2017.
Loughner, C.P., Allen, D.J., Pickering, K.E., Dickerson, R.R., Zhang, D.-L., Shou, Y.-X., 2011. Impact of the Chesapeake Bay breeze and fair-weather cumulus clouds on pollutant transport and transformation. Atmos. Environ. 45, 4060–4072.
Loughner, C.P., Tzortziou, M., Shroder, S., Pickering, K.E., 2016. Enhanced dry deposition of nitrogen pollution near coastlines: a case study covering the Chesapeake Bay estuary and Atlantic Ocean coastline. J. Geophys. Res. Atmos. 121, 14,221–14,238. https://doi.org/10.1002/2016JD025571.
Lucht, W., Schaaf, C.B., Strahler, A.H., 2000. An algorithm for the retrieval of albedo from space using semiempirical BRDF models. IEEE Trans. Geosci. Remote Sens. 38, 977–998. https://doi.org/10.1109/36.841980.
Luo, Y., Yang, X., Carley, R.J., Perkins, C., 2002. Atmospheric deposition of nitrogen along the Connecticut coastline of Long Island Sound: a decade of measurements. Atmos. Environ. 36 (28), 4517–4528.
Ma, S., Tong, D., Lamsal, L., Wang, J., Zhang, X., Tang, Y., Saylor, R., Chai, T., Lee, P., Campbell, P., Baker, B., 2021. Improving predictability of high-ozone episodes through dynamic boundary conditions, emission refresh and chemical data assimilation during the Long Island Sound Tropospheric Ozone Study (LISTOS) field campaign. Atmos. Chem. Phys. 21 (21), 16531–16553.
McLinden, C.A., Olsen, S.C., Hannegan, B., Wild, O., Prather, M.J., Sundet, J., 2000. Stratospheric ozone in 3D models: a simple chemistry and the cross-tropopause flux. J. Geophys. Res.-Atmos. 105, 14653–14665. https://doi.org/10.1029/2000JD900124.
Meir, T., Orton, P.M., Pullen, J., Holt, T., Thompson, W.T., Arend, M.F., 2013. Forecasting the New York City urban heat island and sea breeze during extreme heat events. Weather Forecast. 28 (6), 1460–1477.
Nauth, D., Loughner, C., Tzortziou, M., 2023. The influence of synoptic-scale wind patterns on column-integrated nitrogen dioxide, ground-level ozone, and the development of sea-breeze circulations in the New York City metropolitan area. J. Appl. Meteorol. Climatol. 62 (6), 645–655.
New York Department of Environmental Conservation, 2018. 2018 Press Releases. available at: https://www.dec.ny.gov/press/115749.html (last access: 16 October 2019).
Paerl, H.W., Dennis, R.L., Whitall, D.R., 2002. Atmospheric deposition of nitrogen: implications for nutrient over-enrichment of coastal waters. Estuaries 25, 677–693. https://doi.org/10.1007/BF02804899.
Pardo, L.H., Robin-Abbott, M.J., C.T., 2011. In: D. (Ed.), Assessment of Nitrogen Deposition Effects and Empirical Critical Loads of Nitrogen for Ecoregions of the United States, Gen. Tech. Rep. NRS-80. vol. 80. U.S Department of Agriculture, Forest Service, pp. 1–291. https://doi.org/10.2737/NRS-GTR-80.
Prather, M., 1992. Catastrophic loss of stratospheric ozone in dense volcanic clouds. J. Geophys. Re.-Atmos. 97, 10187–10191. https://doi.org/10.1029/92JD00845.
Reed, A.J., Thompson, A.M., Kollonige, D.E., Martins, D.K., Tzortziou, M.A., Herman, J.R., Berkoff, T.A., Abuhassan, N.K., Cede, A., 2015. Effects of local meteorology and aerosols on ozone and nitrogen dioxide retrievals from OMI and pandora spectrometers in Maryland, USA during DISCOVER-AQ 2011. J. Atmos. Chem. 72 (3), 455–482.
Reuter, M., Buchwitz, M., Schneising, O., Krautwurst, S., O'Dell, C.W., Richter, A., Bovensmann, H., Burrows, J.P., 2019. Towards monitoring localized CO_2 emissions from space: co-located regional CO_2 and NO_2 enhancements observed by the OCO-2 and S5P satellites. Atmos. Chem. Phys. 19, 9371–9383. https://doi.org/10.5194/acp-19-9371-2019.
Roberts-Semple, D., Song, F., Gao, Y., 2012. Seasonal characteristics of ambient nitrogen oxides and ground–level ozone in metropolitan northeastern New Jersey. Atmos. Pollut. Res. 3, 247–257. https://doi.org/10.5094/APR.2012.027.

Rogers, H.M., Ditto, J.C., Gentner, D.R., 2020. Evidence for impacts on surface-level air quality in the northeastern US from long-distance transport of smoke from north American fires during the Long Island Sound Tropospheric Ozone Study (LISTOS) 2018. Atmos. Chem. Phys. 20 (2), 671–682.

Rojas, A.L.P., Venegas, L.E., 2009. Atmospheric deposition of nitrogen emitted in the metropolitan area of Buenos Aires to coastal waters of de la Plata River. Atmos. Environ. 43, 1339–1348.

Rolph, G., Stein, A., Stunder, B., 2017. Real-time environmental applications and display system: READY. Environ. Model Softw. 95, 210–228.

Schaaf, C., Wang, Z., 2015. MCD43A1 MODIS/Terra + Aqua BRDF/Albedo Model Parameters Daily L3 Global – 500m V006, LP DAAC. https://doi.org/10.5067/MODIS/MCD43A1.006.

Spinei, E., Whitehill, A., Fried, A., Tiefengraber, M., Knepp, T.N., Herndon, S., Herman, J.R., Müller, M., Abuhassan, N., Cede, A., Richter, D., Walega, J., Crawford, J., Szykman, J., Valin, L., Williams, D.J., Long, R., Swap, R.J., Lee, Y., Nowak, N., Poche, B., 2018. The first evaluation of formaldehyde column observations by improved Pandora spectrometers during the KORUS-AQ field study. Atmos. Meas. Tech. 11, 4943–4961. https://doi.org/10.5194/amt-11-4943-2018.

Stacey, P.E., Greening, H.S., Kremer, J.N., Peterson, D., Tomasko, D.A., 2001. Contributions of atmospheric nitrogen deposition to U.S. estuaries: summary and conclusions. Nitrogen Loading in Coastal Water Bodies: An Atmospheric Perspective. American Geophysical Union (AGU), pp. 187–226 https://doi.org/10.1029/CE057p0187.

Stajner, I., Davidson, P., Byun, D., McQueen, J., Draxler, R., Dickerson, P., Meagher, J., 2011. US national air quality forecast capability: expanding coverage to include particulate matter. In: Steyn, D.G., Trini Castelli, S. (Eds.), Air Pollution Modeling and its Application. XXI. Springer Netherlands, pp. 379–384.

Stauffer, R.M., Loughner, C.P., Thompson, A.M., 2014. Chesapeake Bay Breeze Enhancement of Air Pollution Episodes and Boundary Layer Venting, EM (in press).

Stein, F.A., Draxler, R.R., Rolph, G.D., Stunder, B.J.B., Cohen, D.M., Ngan, F., 2015. NOAA'S HYSPLIT atmospheric transport and dispersion modeling system. Bull. Am. Meteorol. Soc. 96 (12), 2059–2077. https://doi.org/10.1175/BAMS-D-14-00110.1.

Szykman, J., Swap, R., Lefer, B., Valin, L., Lee, S.C., Fioletov, V., Zhao, X., Davies, J., Williams, D., Abuhassan, N., Shalaby, L., Cede, A., Tiefengraber, M., Mueller, M., Kotsakis, A., Santos, F., Robinson, J., 2019. Pandora: Connecting In-situ and Satellite Monitoring in Support of the Canada - U.S. Air Quality Agreement, EM: Air and Waste Management Association's Magazine for Environmental Managers.

Thompson, W.T., Holt, T., Pullen, J., 2007. Investigation of a sea breeze front in an urban environment. Q. J. R. Meteorol. Soc. 133 (624), 579–594.

Turner, K.J., Tzortziou, M., Grunert, B.K., Goes, J., Sherman, J., 2022. Optical classification of an urbanized estuary using hyperspectral remote sensing reflectance. Opt. Express 30 (23), 41590–41612.

Tzortziou, M., Herman, J.R., Ahmad, Z., Loughner, C.P., Abuhassan, N., Cede, A., 2014. Atmospheric NO2 dynamics and impact on ocean color retrievals in urban nearshore regions. J. Geophys. Res. Oceans 119, 3834–3854. https://doi.org/10.1002/2014JC009803.

Tzortziou, M., Parker, O., Lamb, B., Herman, J.R., Lamsal, L., Stauffer, R., Abuhassan, N., 2018. Atmospheric trace gas (NO2 and O3) variability in south Korean coastal waters, and implications for remote sensing of coastal ocean color dynamics. Remote Sens. 10 (10), 1587. https://doi.org/10.3390/rs10101587.

Tzortziou, M., Kwong, C.F., Goldberg, D., Schiferl, L., Commane, R., Abuhassan, N., Szykman, J.J., Valin, L.C., 2022. Declines and peaks in NO 2 pollution during the multiple waves of the COVID-19 pandemic in the New York metropolitan area. Atmos. Chem. Phys. 22 (4), 2399–2417.

U.S. Census Bureau, 2021. American Community Survey 1-Year Estimates. Retrieved from Census Reporter Profile page for New York-Newark-Jersey City, NY-NJ-PA Metro Area. http://censusreporter.org/profiles/31000US35620-new-york-newark-jersey-city-ny-nj-pa-metro-area/.

U.S. EPA, 2016. Integrated science assessment for oxides of nitrogen – health criteria (final report) (EPA/600/R-15/068), January 2016. www.epa.gov/isa.

Veefkind, J.P., Aben, I., McMullan, K., Förster, H., de Vries, J., Otter, G., Claas, J., Eskes, H.J., de Haan, J.F., Kleipool, Q., van Weele, M., Hasekamp, O., Hoogeveen, R., Landgraf, J., Snel, R., Tol, P., Ingmann, P., Voors, R., Kruizinga, B., Vink, R., Visser, H., Levelt, P.F., 2012. TROPOMI on the ESA Sentinel-5 precursor: a GMES mission for global observations of the atmospheric composition for climate, air quality and ozone layer applications. Remote Sens. Environ. 120, 70–83. https://doi.org/10.1016/j.rse.2011.09.027.

Verhoelst, T., Compernolle, S., Pinardi, G., Lambert, J.-C., Eskes, H.J., Eichmann, K.-U., Fjæraa, A.M., Granville, J., Niemeijer, S., Cede, A., Tiefengraber, M., Hendrick, F., Pazmiño, A., Bais, A., Bazureau, A., Boersma, K.F., Bognar, K., Dehn, A., Donner, S., Elokhov, A., Gebetsberger, M., Goutail, F., Grutter de la Mora, M., Gruzdev, A., Gratsea, M., Hansen, G.H., Irie, H., Jepsen, N., Kanaya, Y., Karagkiozidis, D., Kivi, R., Kreher, K., Levelt, P.F., Liu, C., Müller, M., Navarro Comas, M., Piters, A.J.M., Pommereau, J.-P., Portafaix, T., Prados-Roman, C., Puentedura, O., Querel, R., Remmers, J., Richter, A., Rimmer, J., Rivera Cárdenas, C., Saavedra de Miguel, L., Sinyakov, V.P., Stremme, W., Strong, K., Van Roozendael, M., Veefkind, J.P., Wagner, T., Wittrock, F., Yela González, M., Zehner, C., 2021. Ground-based validation of the Copernicus sentinel-5P TROPOMI NO_2 measurements with the NDACC ZSL-DOAS, MAX-DOAS and Pandonia global networks. Atmos. Meas. Tech. 14, 481–510. https://doi.org/10.5194/amt-14-481-2021.

Wu, Y., Nehrir, A.R., Ren, X., Dickerson, R.R., Huang, J., Stratton, P.R., Gronoff, G., Kooi, S.A., Collins, J.E., Berkoff, T.A., Lei, L., 2021. Synergistic aircraft and ground observations of transported wildfire smoke and its impact on air quality in new York City during the summer 2018 LISTOS campaign. Sci. Total Environ. 773, 145030.

Zhang, D.L., Shou, Y.X., Dickerson, R.R., 2009. Upstream urbanization exacerbates urban heat island effects. Geophys. Res. Lett. 36, L24401. https://doi.org/10.1029/2009GL041082, 2009.

Zhang, J., Ninneman, M., Joseph, E., Schwab, M.J., Shrestha, B., Schwab, J.J., 2020. Mobile laboratory measurements of high surface ozone levels and spatial heterogeneity during LISTOS 2018: evidence for sea breeze influence. J. Geophys. Res. Atmos. 125 (11), e2019JD031961.

Zhang, J., Mak, J., Wei, Z., Cao, C., Ninneman, M., Marto, J., Schwab, J.J., 2021. Long Island enhanced aerosol event during 2018 LISTOS: association with heatwave and marine influences. Environ. Pollut. 270, 116299.

Zhao, X., Griffin, D., Fioletov, V., McLinden, C., Cede, A., Tiefengraber, M., Müller, M., Bognar, K., Strong, K., Boersma, F., Eskes, H., Davies, J., Ogyu, A., Lee, S.C., 2020. Assessment of the quality of TROPOMI high-spatial-resolution NO_2 data products in the Greater Toronto Area. Atmos. Meas. Tech. 13, 2131–2159. https://doi.org/10.5194/amt-13-2131-2020.